

Inflationary susceptibilities, duality and large-scale magnetic fields generation

Massimo Giovannini ¹

Department of Physics, Theory Division, CERN, 1211 Geneva 23, Switzerland

INFN, Section of Milan-Bicocca, 20126 Milan, Italy

Abstract

We investigate what can be said about the interaction of scalar fields with Abelian gauge fields during a quasi-de Sitter phase of expansion and under the assumption that the electric and the magnetic susceptibilities do not coincide. The duality symmetry, transforming the magnetic susceptibility into the inverse of the electric susceptibility, exchanges the magnetic and electric power spectra. The mismatch between the two susceptibilities determines an effective refractive index affecting the evolution of the canonical fields. The constraints imposed by the duration of the inflationary phase and by the magnetogenesis requirements pin down the rate of variation of the susceptibilities that is consistent with the observations of the magnetic field strength over astrophysical and cosmological scales but avoids back-reaction problems. The parameter space of this magnetogenesis scenario is wider than in the case when the susceptibilities are equal, as it happens when the inflaton or some other spectator field is solely coupled to the standard gauge kinetic term.

¹Electronic address: massimo.giovannini@cern.ch

1 Introduction

Large-scale magnetic field generation may take place in the early Universe [1, 2, 3] and there are plausible reasons for this conjecture dubbed, some time ago, magnetogenesis [4]. In this framework specific attention has been devoted to the interaction of gauge fields with scalar degrees of freedom during a quasi-de Sitter phase of expansion and in more general curved backgrounds relevant to cosmology (see, e.g. [5, 6, 7, 8, 9, 10, 11, 12] for a non exhaustive list of references). The temperature and polarization anisotropies of the Cosmic Microwave Background (CMB in what follows) offer important clues about the origin of large-scale magnetism as repeatedly argued, along different perspectives (see e.g. [1, 2, 3, 4]), during the past score year. A complete computation of the CMB observables has been recently presented [13] under the hypothesis that the same inflationary seed accounting for protogalactic magnetism also affects the EinsteinBoltzmann hierarchy whose initial conditions have been directly bootstrapped out of the values provided by inflationary magnetogenesis.

The aim of the present study is to discuss the idea that the electric and the magnetic susceptibilities may not coincide during inflation. So far such a possibility did not receive specific attention. For sake of definiteness consider the following action:

$$S = -\frac{1}{16\pi} \int d^4x \sqrt{-g} \left[\lambda(\varphi, \psi) Y_{\alpha\beta} Y^{\alpha\beta} + \mathcal{M}_\sigma^\rho(\varphi) Y_{\rho\alpha} Y^{\sigma\alpha} - \mathcal{N}_\sigma^\rho(\psi) \tilde{Y}_{\rho\alpha} \tilde{Y}^{\sigma\alpha} \right], \quad (1.1)$$

where $Y^{\mu\nu}$ and $\tilde{Y}^{\mu\nu}$ are, respectively, the gauge field strength and its dual; $g = \det g_{\mu\nu}$ is the determinant of the four-dimensional metric with signature mostly minus. In the conventional case (see e.g. [5, 6, 7, 8, 9, 10, 11, 12]) \mathcal{M}_σ^ρ and \mathcal{N}_σ^ρ are absent from Eq. (1.1) so that the only coupling of the gauge fields to the scalar degrees of freedom is encoded in the first term inside the square bracket on the right hand side of Eq. (1.1). Suppose, as an example, that \mathcal{M}_σ^ρ and \mathcal{N}_σ^ρ take the following form:

$$\begin{aligned} \mathcal{M}_\sigma^\rho(\varphi) &= \frac{1}{2} \left(\partial_\sigma m_E^* \partial^\rho m_E + \partial_\sigma m_E \partial^\rho m_E^* \right), \\ \mathcal{N}_\sigma^\rho(\psi) &= \frac{1}{2} \left(\partial_\sigma n_B^* \partial^\rho n_B + \partial_\sigma n_B \partial^\rho n_B^* \right), \end{aligned} \quad (1.2)$$

where $m_E = m_E(\varphi)$ and $n_B = n_B(\psi)$. More complicated possibilities can be certainly imagined, like for instance $m_E = m_E(\varphi, \psi, \dots)$ and $n_B = n_B(\varphi, \psi, \dots)$; the ellipses stand for other supplementary fields in case there are various inflatons or more than one spectator field [14]. Equations (1.1)–(1.2) describe the situation where the electric and the magnetic susceptibilities are not equal and include, as a special case, the following interaction

$$S = - \int d^4x \sqrt{-g} \left[g_1 \partial_\alpha \varphi \partial_\beta \varphi^* Y^{\alpha\rho} Y_\rho^\beta + g_2 |\varphi|^2 Y_{\alpha\beta} Y^{\alpha\beta} \right], \quad (1.3)$$

that appears in the relativistic theory of Casimir-Polder and Van der Waals forces [15]. Equation (1.3) leads to static electric and magnetic susceptibilities that effectively depend

on the scalar degrees of freedom; in the present study, the electric and the magnetic susceptibilities will be dynamical rather than static but still this analogy is physically instructive. Two further terms may arise in Eq. (1.1)

$$S = -\frac{1}{16\pi} \int d^4x \sqrt{-g} \left[\bar{\lambda}(\psi) Y_{\alpha\beta} \tilde{Y}^{\alpha\beta} + \overline{\mathcal{M}}_\sigma^\rho(\psi) Y_{\rho\alpha} \tilde{Y}^{\sigma\alpha} \right], \quad (1.4)$$

where ψ may or may not coincide with the degrees of freedom mentioned above. In the simplest case $\overline{\mathcal{M}}_\sigma^\rho = 0$ and $\bar{\lambda} = \psi/M$: this is in a nutshell the coupling to the axions [16] which is not so effective for the amplification of gauge field fluctuations during a quasi-de Sitter stage of expansion [17, 18, 19]. The pseudo-scalar vertex changes the topology of the magnetic flux lines once gauge field fluctuations have been already amplified [20]. For this reason the interactions appearing in Eq. (1.4) shall be neglected at least for the purposes of the present study.

If \mathcal{M}_ρ^σ and \mathcal{N}_ρ^σ are absent from Eq. (1.1), the corresponding canonical Hamiltonian is explicitly invariant under electromagnetic duality [21, 22] when $\sqrt{\lambda} \rightarrow 1/\sqrt{\lambda}$. In practice this symmetry exchanges the magnetic and electric power spectra produced during a phase of quasi-de Sitter expansion and, more generally, in conformally flat backgrounds [22]. Whenever \mathcal{M}_ρ^σ and \mathcal{N}_ρ^σ are present a generalized duality symmetry transforms the magnetic susceptibility into the inverse of the electric susceptibility (and vice versa).

The dynamical difference between electric and magnetic susceptibility affects the amplification of the quantum fluctuations of the gauge fields whose power spectra are related by duality. The computed power spectra can then be examined in the light of the magnetogenesis requirements and of other back-reaction constraints. The main purpose of this paper is not to endorse a specific set of initial conditions but to provide a comprehensive analysis of the whole idea. The parameter space of the model is wider than in the conventional case; both strongly and weakly coupled initial conditions are possible.

The paper is organized as follows. In section 2, after some technical generalities, we introduce the electric and the magnetic susceptibilities in conformally flat backgrounds and discuss the duality symmetry of the system. Section 3 is devoted to the quantization of the problem and to the amplification of the quantum fluctuations of the gauge fields. The non-trivial evolution equations of the mode functions are solved in section 4; the power spectra are explicitly computed and related via the duality symmetry. Section 5 contains the phenomenological considerations related to magnetogenesis. The concluding remarks are collected in section 6.

2 Generalities

2.1 Preliminary considerations

From the action (1.1) the following equations of motion can be easily derived:

$$\nabla_\alpha \left(\lambda Y^{\alpha\beta} \right) + \frac{1}{2} \nabla_\alpha \mathcal{Z}^{\alpha\beta} - \frac{1}{2} \nabla_\alpha \mathcal{W}^{\alpha\beta} = 4\pi j^\beta, \quad (2.1)$$

$$\nabla_\alpha \tilde{Y}^{\alpha\beta} = 0, \quad (2.2)$$

where ∇_α is the covariant derivative; the two antisymmetric tensors $\mathcal{Z}^{\alpha\beta}$ and $\mathcal{W}^{\alpha\beta}$ are:

$$\mathcal{Z}^{\alpha\beta} = \mathcal{M}_\sigma^\alpha Y^{\sigma\beta} - \mathcal{M}_\sigma^\beta Y^{\sigma\alpha}, \quad (2.3)$$

$$\mathcal{W}^{\alpha\beta} = E^{\alpha\beta\rho\zeta} \tilde{Y}_{\sigma\zeta} \mathcal{N}_\rho^\sigma \quad (2.4)$$

$$= \mathcal{N}_\rho^\beta Y^{\alpha\rho} - \mathcal{N}_\rho^\alpha Y^{\beta\rho} - \mathcal{N}_\rho^\rho Y^{\alpha\beta}. \quad (2.5)$$

In Eq. (2.4) $E^{\alpha\beta\rho\zeta} = \epsilon^{\alpha\beta\rho\zeta} / \sqrt{-g}$ and $\epsilon^{\alpha\beta\rho\zeta}$ is the total antisymmetric pseudotensor of fourth rank. Equations (2.1) and (2.2) can also be recast in the following form:

$$\frac{1}{\sqrt{-g}} \partial_\alpha \left[\sqrt{-g} \lambda Y^{\alpha\beta} \right] + \frac{1}{2\sqrt{-g}} \partial_\alpha \left[\sqrt{-g} \mathcal{Z}^{\alpha\beta} \right] - \frac{1}{2\sqrt{-g}} \partial_\alpha \left[\sqrt{-g} \mathcal{W}^{\alpha\beta} \right] = 4\pi j^\beta, \quad (2.6)$$

$$\frac{1}{\sqrt{-g}} \partial_\alpha \left[\sqrt{-g} \tilde{Y}^{\alpha\beta} \right] = 0. \quad (2.7)$$

The tensors \mathcal{M}_σ^ρ and of \mathcal{N}_σ^ρ shall now be parametrized as:

$$\mathcal{M}_\sigma^\rho(\varphi) = \lambda_E(\varphi) u^\rho u_\sigma, \quad \mathcal{N}_\sigma^\rho(\psi) = \lambda_B(\psi) \bar{u}^\rho \bar{u}_\sigma, \quad (2.8)$$

where

$$u_\rho = \frac{\partial_\rho \varphi}{\sqrt{g^{\alpha\beta} \partial_\alpha \varphi \partial_\beta \varphi}}, \quad \bar{u}_\rho = \frac{\partial_\rho \psi}{\sqrt{g^{\alpha\beta} \partial_\alpha \psi \partial_\beta \psi}}, \quad (2.9)$$

and $g^{\alpha\beta} u_\alpha u_\beta = 1$, $g^{\alpha\beta} \bar{u}_\alpha \bar{u}_\beta = 1$. The validity of the parametrization (2.8) can be verified by inserting, for instance², $m_E(\varphi) = \exp(\theta_\varphi \varphi / M_\varphi)$ and $n_B(\psi) = \exp(\theta_\psi \psi / M_\psi)$ into Eq. (1.2). Equation (2.8) implies that u_μ and \bar{u}_μ are invariant under the reparametrizations of φ and ψ , i.e. $\varphi \rightarrow \Phi = q_1(\varphi)$ and $\psi \rightarrow \Psi = q_2(\psi)$. For these reasons different models may lead to the same λ_E and λ_B and the parametrization of Eq. (2.8) is sufficiently general for the present ends. Using Eq. (2.8) the action (1.1) can be recast in the following form:

$$S = -\frac{1}{16\pi} \int d^4x \sqrt{-g} \left[\lambda Y_{\alpha\beta} Y^{\alpha\beta} + \lambda_E u^\rho u_\sigma Y_{\rho\alpha} Y^{\sigma\alpha} - \lambda_B \bar{u}^\rho \bar{u}_\sigma \tilde{Y}_{\rho\alpha} \tilde{Y}^{\sigma\alpha} \right]. \quad (2.10)$$

Equation (2.10) elucidates the connection of λ_E and λ_B with the electric and magnetic susceptibilities. In fact $u_\rho \tilde{Y}^{\alpha\rho} = \mathcal{B}^\alpha$ and $u_\rho Y^{\alpha\rho} = \mathcal{E}^\alpha$ are the electric and magnetic fields

²Note that θ_φ and θ_ψ are dimensionless constants while M_φ and M_ψ are two different mass scales.

in covariant form as it follows from the generally covariant decomposition of the gauge field strengths [23]:

$$\begin{aligned} Y_{\alpha\beta} &= \mathcal{E}_\alpha u_\beta - \mathcal{E}_\beta u_\alpha + E_{\alpha\beta\rho\sigma} u^\rho \mathcal{B}^\sigma, \\ \tilde{Y}^{\alpha\beta} &= \mathcal{B}^\alpha u^\beta - \mathcal{B}^\beta u^\alpha + E^{\alpha\beta\rho\sigma} \mathcal{E}_\rho u_\sigma, \end{aligned} \quad (2.11)$$

where the four-velocity may coincide either with u_ρ or with \bar{u}_ρ . The functional \mathcal{M}_ρ^σ and \mathcal{N}_ρ^σ can be split into a homogeneous part and an inhomogeneous part, i.e.

$$\begin{aligned} \mathcal{M}_0^0(\tau) &= \lambda_E(\tau) u_0 u^0, & \mathcal{N}_0^0(\tau) &= \lambda_B(\tau) \bar{u}_0 \bar{u}^0, \\ \mathcal{M}_i^0(\vec{x}, \tau) &= \lambda_E^{(1)}(\vec{x}, \tau) u_i u^0, & \mathcal{N}_i^0(\vec{x}, \tau) &= \lambda_B^{(1)}(\vec{x}, \tau) \bar{u}_i \bar{u}^0, \\ \mathcal{M}_i^j(\vec{x}, \tau) &= \lambda_E^{(1)}(\vec{x}, \tau) u_i u^j, & \mathcal{N}_i^j(\vec{x}, \tau) &= \lambda_B^{(1)}(\vec{x}, \tau) \bar{u}_i \bar{u}^j, \end{aligned} \quad (2.12)$$

where $\lambda_E(\vec{x}, \tau) = \lambda_E(\tau) + \lambda_E^{(1)}(\vec{x}, \tau)$ and $\lambda_B(\vec{x}, \tau) = \lambda_B(\tau) + \lambda_B^{(1)}(\vec{x}, \tau)$. The various contributions can be taken into account, order by order, within the standard perturbative expansion involving the fluctuations of the scalar degrees of freedom and of the geometry³. Finally, from the action (1.1) the energy-momentum tensor of the gauge fields reads:

$$T_\mu^\nu = \frac{1}{4\pi} \left[-\mathcal{S}_\mu^\nu + \frac{1}{4} \mathcal{S} \delta_\mu^\nu \right], \quad (2.13)$$

where

$$\begin{aligned} \mathcal{S}_\mu^\nu &= \lambda Y_{\alpha\mu} Y^{\alpha\nu} + \frac{1}{2} \left(\mathcal{M}_\mu^\rho Y_{\rho\alpha} Y^{\nu\alpha} + \mathcal{M}_\sigma^\rho Y_{\rho\mu} Y^{\sigma\nu} \right) \\ &- \frac{1}{2} \left(\mathcal{N}_\mu^\rho \tilde{Y}_{\rho\alpha} \tilde{Y}^{\nu\alpha} + \mathcal{N}_\sigma^\rho \tilde{Y}_{\rho\mu} \tilde{Y}^{\sigma\nu} \right). \end{aligned} \quad (2.14)$$

2.2 Conformally flat backgrounds

Consider the case of a conformally flat metric $g_{\mu\nu} = a^2(\tau) \eta_{\mu\nu}$ where $a(\tau)$ is the scale factor and $\eta_{\mu\nu}$ is the Minkowski metric. To lowest order $\mathcal{M}_0^0(\tau) = \lambda_E(\tau)$ and $\mathcal{N}_0^0(\tau) = \lambda_B(\tau)$ are homogeneous (see Eq. (2.12)) while all the other entries are inhomogeneous. Recalling that $Y^{i0} = e^i/a^2$ and $Y^{ij} = -\epsilon^{ijk} b_k/a^2$ (where \vec{e} and \vec{b} are the electric and magnetic fields in flat space-time), Eqs. (2.1)–(2.2) and (2.6)–(2.7) can be written as:

$$\begin{aligned} \vec{\nabla} \cdot \left[a^2 \left(\lambda + \frac{\lambda_E}{2} \right) \vec{e} \right] &= 4\pi\rho, \\ \vec{\nabla} \times \left[a^2 \left(\lambda + \frac{\lambda_B}{2} \right) \vec{b} \right] &= \partial_\tau \left[a^2 \left(\lambda + \frac{\lambda_E}{2} \right) \vec{e} \right] + 4\pi \vec{J}, \\ \vec{\nabla} \cdot (a^2 \vec{b}) &= 0, \quad \partial_\tau (a^2 \vec{b}) + \vec{\nabla} \times (a^2 \vec{e}) = 0, \end{aligned} \quad (2.15)$$

³The leading order contribution of Eq. (2.12), i.e. the fully homogeneous part, is, in a sense, more general than the original action insofar as it can even parametrize the case where the interaction is not in the form of Eq. (1.2); some examples along this direction are $\partial^\rho \partial_\sigma \varphi Y_{\rho\alpha} Y^{\sigma\alpha}$ or $\partial^\rho \partial_\sigma \psi \tilde{Y}_{\rho\alpha} \tilde{Y}^{\sigma\alpha}$.

where ρ and \vec{J} denote the electromagnetic sources that are important both at the beginning and at the end of the inflationary evolution⁴. Introducing the following rescaled fields

$$\vec{B} = a^2 \sqrt{\Lambda_B} \vec{b}, \quad \vec{E} = a^2 \sqrt{\Lambda_E} \vec{e}, \quad (2.16)$$

$$\Lambda_B = \lambda + \frac{\lambda_B}{2}, \quad \Lambda_E = \lambda + \frac{\lambda_E}{2}, \quad (2.17)$$

the system of Eq. (2.15) becomes:

$$\vec{\nabla} \times \left(\sqrt{\Lambda_B} \vec{B} \right) = \partial_\tau \left(\sqrt{\Lambda_E} \vec{E} \right) + 4\pi \vec{J}, \quad (2.18)$$

$$\vec{\nabla} \times \left(\frac{\vec{E}}{\sqrt{\Lambda_E}} \right) + \partial_\tau \left(\frac{\vec{B}}{\sqrt{\Lambda_B}} \right) = 0, \quad (2.19)$$

$$\vec{\nabla} \cdot \left(\frac{\vec{B}}{\sqrt{\Lambda_B}} \right) = 0, \quad \vec{\nabla} \cdot (\sqrt{\Lambda_E} \vec{E}) = 4\pi \rho. \quad (2.20)$$

The electric and the magnetic susceptibilities χ_E and χ_B are defined as:

$$\chi_E = \sqrt{\Lambda_E} \equiv \sqrt{f \Lambda_B}, \quad \chi_B = \sqrt{\Lambda_B} \equiv \sqrt{\frac{\Lambda_E}{f}}, \quad f = \left(\frac{\chi_E}{\chi_B} \right)^2 = \frac{\Lambda_E}{\Lambda_B}. \quad (2.21)$$

From the Eqs. (2.13)–(2.14) it is possible to deduce the various components of the energy-momentum tensor by recalling the relation of the gauge field strengths to the physical fields. Consider, for instance, the energy density always in the case of the general parametrization discussed above

$$T_0^0 = \frac{1}{8\pi} \left[\chi_E e^2 + \chi_B b^2 \right], \quad (2.22)$$

which can be expressed in terms of the rescaled fields \vec{E} and \vec{B} , when needed. Similar manipulations can be used to deduce the other components of the energy-momentum tensor.

2.3 Duality properties

Neglecting the sources, Eqs. (2.18), (2.19) and (2.20) are invariant under the following set of transformations:

$$\vec{E} \rightarrow -\vec{B}, \quad \vec{B} \rightarrow \vec{E}, \quad \chi_B \rightarrow \frac{1}{\chi_E}, \quad \chi_E \rightarrow \frac{1}{\chi_B}, \quad (2.23)$$

leaving unaltered the ratio $f = (\chi_E/\chi_B)^2$. The duality properties are manifest from the decoupled evolution of the electric and of the magnetic fields:

$$\frac{1}{\chi_B} \partial_\tau \left[\chi_E^2 \partial_\tau \left(\frac{\vec{B}}{\chi_B} \right) \right] - \nabla^2 \vec{B} = \frac{4\pi}{\chi_B} \vec{\nabla} \times \vec{J}, \quad (2.24)$$

$$\chi_E \partial_\tau \left[\frac{1}{\chi_B^2} \partial_\tau \left(\chi_E \vec{E} \right) + \frac{4\pi}{\chi_B^2} \vec{J} \right] - \nabla^2 \vec{E} = 0. \quad (2.25)$$

⁴During the protoinflationary stage of expansion, the electromagnetic sources are not immediately washed out because there exist symmetries preventing their dissipation [12]. At the end of inflation charged particles must be included as they determine the effective post-inflationary conductivity. The total charge density vanishes on its own since the initial plasma, even if present, must be globally neutral.

Equations (2.24) and (2.25) can be written, more explicitly, as:

$$\vec{E}'' + 2\left(\frac{\chi_E}{\chi_B}\right)' \left(\frac{\chi_B}{\chi_E}\right) \vec{E}' + \left[\frac{\chi_E''}{\chi_E} - 2\left(\frac{\chi_E'}{\chi_E}\right)\left(\frac{\chi_B'}{\chi_B}\right)\right] \vec{E} - \frac{\nabla^2 \vec{E}}{f} = -4\pi \frac{\chi_E}{f} \left(\frac{\vec{J}}{\chi_B}\right)', \quad (2.26)$$

$$\vec{B}'' + 2\left(\frac{\chi_E}{\chi_B}\right)' \left(\frac{\chi_B}{\chi_E}\right) \vec{B}' + \left[\chi_B \left(\frac{1}{\chi_B}\right)'' - 2\left(\frac{\chi_E'}{\chi_E}\right)\left(\frac{\chi_B'}{\chi_B}\right)\right] \vec{B} - \frac{\nabla^2 \vec{B}}{f} = \frac{4\pi \vec{\nabla} \times \vec{J}}{\chi_B f}, \quad (2.27)$$

where the prime denotes a derivation with respect to the conformal time coordinate τ . Recalling Eq. (2.23), the system of Eqs. (2.26) and (2.27) is left invariant by Eq. (2.23) provided $\vec{J} = 0$. Using a further rescaling of the electric and magnetic fields (i.e. $\vec{Q}_B = \sqrt{f} \vec{B}$ and $\vec{Q}_E = \sqrt{f} \vec{E}$), Eqs. (2.26) and (2.27) can be simplified by eliminating the first time derivatives:

$$\vec{Q}_B'' - \frac{\nabla^2 \vec{Q}_B}{f} - \frac{(\chi_B \sqrt{f})''}{\chi_B \sqrt{f}} \vec{Q}_B = \frac{4\pi \vec{\nabla} \times \vec{J}}{\chi_B \sqrt{f}}, \quad (2.28)$$

$$\vec{Q}_E'' - \frac{\nabla^2 \vec{Q}_E}{f} - \left(\frac{\sqrt{f}}{\chi_E}\right)'' \left(\frac{\chi_E}{f}\right) \vec{Q}_E = -\frac{4\pi \chi_E}{\sqrt{f}} \left(\frac{\vec{J}}{\chi_B^2}\right)'. \quad (2.29)$$

From Eq. (2.16) we have that $\vec{B} = a^2 \vec{\nabla} \times (\chi_B \vec{Y})$ and $\vec{E} = -\chi_E \partial_\tau \vec{Y}$ where \vec{Y} is the vector potential in the gauge $Y_0 = 0$ and $\vec{\nabla} \cdot \vec{Y} = 0$. As specifically discussed in the section 3, the canonical normal mode of the action is related to the vector potential \vec{Y} as $\vec{Y} = \vec{A}/\chi_E$ up to a constant that depends on the system of units. Consequently the relation of the electric and magnetic fields to the canonical vector potential is:

$$\vec{B} = \vec{\nabla} \times \left(\frac{\chi_B}{\chi_E} \vec{A}\right) = \vec{\nabla} \times \left(\frac{\vec{A}}{\sqrt{f}}\right), \quad (2.30)$$

$$\vec{E} = -\chi_E \left(\frac{\vec{A}}{\chi_E}\right)' = -\vec{A}' + \frac{\chi_E'}{\chi_E} \vec{A}. \quad (2.31)$$

Inserting Eqs. (2.30) and (2.31) into Eq. (2.18) the equation obeyed by \vec{A} can be obtained and solved; this analysis will be postponed to sections 3 and 4. It is finally useful to discuss, in some detail, the limit $\chi_E \rightarrow \chi_B$ (or, which is the same, $f \rightarrow 1$). When $f \rightarrow 1$ the following relations can be explicitly verified:

$$\lim_{f \rightarrow 1} \chi_B = \lim_{f \rightarrow 1} \chi_E = \sqrt{\lambda}, \quad \lim_{f \rightarrow 1} \vec{Q}_B = \vec{B}, \quad \lim_{f \rightarrow 1} \vec{Q}_E = \vec{E}. \quad (2.32)$$

Using Eq. (2.32) into Eqs. (2.28) and (2.29) we obtain

$$\vec{B}'' - \nabla^2 \vec{B} - \frac{\sqrt{\lambda}''}{\sqrt{\lambda}} \vec{B} = \frac{4\pi \vec{\nabla} \times \vec{J}}{\sqrt{\lambda}}, \quad (2.33)$$

$$\vec{E}'' - \nabla^2 \vec{E} - \left(\frac{1}{\sqrt{\lambda}}\right)'' \sqrt{\lambda} \vec{E} = -4\pi \sqrt{\lambda} \left(\frac{\vec{J}}{\lambda}\right)', \quad (2.34)$$

which is the standard result obtainable in the case when $\mathcal{M}_\rho^\sigma \rightarrow 0$ and $\mathcal{N}_\rho^\sigma \rightarrow 0$ in Eq. (1.1) (see, for instance, [12, 22]).

3 Quantum fluctuations

3.1 Canonical Hamiltonian

Consider Eqs. (1.1) and (2.10), in time-dependent (conformally flat) backgrounds and in the Coulomb gauge (i.e. $Y_0 = 0$ and $\vec{\nabla} \cdot \vec{Y} = 0$) that is preserved (unlike the Lorentz gauge condition) under a conformal rescaling of the metric. The action (2.10) becomes:

$$S = \int d\tau L(\tau), \quad L(\tau) = \int d^3x \mathcal{L}(\vec{x}, \tau), \quad (3.1)$$

$$\mathcal{L}(\vec{x}, \tau) = \frac{1}{2} \left\{ \vec{A}'^2 + \left(\frac{\chi'_E}{\chi_E} \right)^2 \vec{A}^2 - 2 \frac{\chi'_E}{\chi_E} \vec{A} \cdot \vec{A}' - \frac{\chi_B^2}{\chi_E^2} \partial_i \vec{A} \cdot \partial^i \vec{A} \right\}, \quad (3.2)$$

where⁵ $\vec{A} = \sqrt{\Lambda_E/(4\pi)} \vec{Y}$. We have assumed that χ_E and χ_B are only dependent on the conformal time coordinate τ . The canonical momentum conjugate to \vec{A} is obtained from Eq. (3.2) and it coincides, up to a sign, with the canonical electric field, i.e.

$$\vec{\pi} = \vec{A}' - \frac{\chi'_E}{\chi_E} \vec{A} = -\vec{E}, \quad (3.3)$$

while, as already discussed, $\vec{B} = \vec{\nabla} \times (\vec{A}/\sqrt{f})$. The canonical Hamiltonian is then given by

$$H_A(\tau) = \frac{1}{2} \int d^3x \left[\vec{\pi}^2 + 2 \frac{\chi'_E}{\chi_E} \vec{\pi} \cdot \vec{A} + \frac{\partial_i \vec{A} \cdot \partial^i \vec{A}}{f} \right]. \quad (3.4)$$

Since χ_E , χ_B and f are not three independent functions, only two of them can be independently assigned. It is practical to select χ_E and f independently while χ_B can be derived as $\chi_B = \chi_E/\sqrt{f}$. The Fourier mode expansion for the canonical fields reads

$$\vec{\pi}(\vec{x}, \tau) = \frac{1}{(2\pi)^{3/2}} \int d^3k \vec{\pi}_{\vec{k}}(\tau) e^{-i\vec{k} \cdot \vec{x}}, \quad \vec{A}(\vec{x}, \tau) = \frac{1}{(2\pi)^{3/2}} \int d^3k \vec{A}_{\vec{k}}(\tau) e^{-i\vec{k} \cdot \vec{x}}, \quad (3.5)$$

and it can be inserted into Eq. (3.4). The resulting form of the canonical Hamiltonian is:

$$H_A(\tau) = \frac{1}{2} \int d^3k \left[\vec{\pi}_{\vec{k}} \cdot \vec{\pi}_{-\vec{k}} + \frac{\chi'_E}{\chi_E} \left(\vec{\pi}_{\vec{k}} \cdot \vec{A}_{-\vec{k}} + \vec{\pi}_{-\vec{k}} \cdot \vec{A}_{\vec{k}} \right) + \frac{k^2}{f} \vec{A}_{\vec{k}} \cdot \vec{A}_{-\vec{k}} \right]. \quad (3.6)$$

From Eq. (3.6) the corresponding equations of motion are:

$$\vec{A}'_{\vec{k}} = \vec{\pi}_{\vec{k}} + \frac{\chi'_E}{\chi_E} \vec{A}_{\vec{k}}, \quad (3.7)$$

$$\vec{\pi}'_{\vec{k}} = -\frac{k^2}{f} \vec{A}_{\vec{k}} - \frac{\chi'_E}{\chi_E} \vec{\pi}_{\vec{k}}. \quad (3.8)$$

⁵The $1/\sqrt{4\pi}$ is purely conventional and its presence comes from the factor 16π included in the initial gauge action of Eq. (1.1).

The duality transformation exchanges the canonical fields and the conjugate momenta

$$\begin{aligned}\chi_E &\rightarrow \frac{1}{\chi_B}, & \chi_B &\rightarrow \frac{1}{\chi_E}, \\ \vec{\pi}_{\vec{k}} &\rightarrow \Pi_{\vec{k}} = -\frac{k}{\sqrt{f}} \vec{A}_{\vec{k}}, & \vec{A}_{\vec{k}} &\rightarrow \vec{\mathcal{A}}_{\vec{k}} = \frac{\sqrt{f}}{k} \vec{\pi}_{\vec{k}},\end{aligned}\quad (3.9)$$

and it also replaces Eq. (3.7) with Eq. (3.8) and vice versa. The transformation of Eq. (3.9) is canonical and the generating functional can be written as:

$$\mathcal{G}[\vec{A}, \vec{\mathcal{A}}, \tau] = \int d^3k \frac{k}{\sqrt{f(\tau)}} \left(\vec{\mathcal{A}}_{\vec{k}} \cdot \vec{A}_{\vec{k}} + \vec{\mathcal{A}}_{-\vec{k}} \cdot \vec{A}_{-\vec{k}} \right). \quad (3.10)$$

The transformed Hamiltonian will be given by

$$\begin{aligned}H_A(\tau) &\rightarrow \overline{H}_A = H_A + \frac{\partial \mathcal{G}}{\partial \tau} \\ &= \frac{1}{2} \int d^3k \left[\vec{\Pi}_{\vec{k}} \cdot \vec{\Pi}_{-\vec{k}} + \frac{\chi'_E}{\chi_E} \left(\vec{\Pi}_{\vec{k}} \cdot \vec{\mathcal{A}}_{-\vec{k}} + \vec{\Pi}_{-\vec{k}} \cdot \vec{\mathcal{A}}_{\vec{k}} \right) + \frac{k^2}{f} \vec{\mathcal{A}}_{\vec{k}} \cdot \vec{\mathcal{A}}_{-\vec{k}} \right],\end{aligned}\quad (3.11)$$

where we have used the identity $\chi'_E/\chi_E = (\chi'_B/\chi_B + \sqrt{f'}/\sqrt{f})$.

3.2 Mode functions and power spectra

Promoting the canonical fields to quantum operators (i.e. $A_i \rightarrow \hat{A}_i$ and $\pi_i \rightarrow \hat{\pi}_i$) the following (equal time) commutation relations (in units $\hbar = c = 1$) must hold:

$$[\hat{A}_i(\vec{x}_1, \tau), \hat{\pi}_j(\vec{x}_2, \tau)] = i\Delta_{ij}(\vec{x}_1 - \vec{x}_2), \quad \Delta_{ij}(\vec{x}_1 - \vec{x}_2) = \int \frac{d^3k}{(2\pi)^3} e^{i\vec{k} \cdot (\vec{x}_1 - \vec{x}_2)} P_{ij}(k), \quad (3.12)$$

where $P_{ij}(k) = (\delta_{ij} - k_i k_j / k^2)$. The function $\Delta_{ij}(\vec{x}_1 - \vec{x}_2)$ is the transverse generalization of the Dirac delta function ensuring that both \vec{E} and \vec{A} are divergenceless. The field operators can then be expanded in terms of the corresponding mode functions

$$\hat{A}_i(\vec{x}, \tau) = \int \frac{d^3k}{(2\pi)^{3/2}} \sum_{\alpha} e_i^{(\alpha)}(k) \left[F_k(\tau) \hat{a}_{k,\alpha} e^{-i\vec{k} \cdot \vec{x}} + F_k^*(\tau) \hat{a}_{k,\alpha}^\dagger e^{i\vec{k} \cdot \vec{x}} \right], \quad (3.13)$$

$$\hat{\pi}_i(\vec{x}, \tau) = \int \frac{d^3k}{(2\pi)^{3/2}} \sum_{\alpha} e_i^{(\alpha)}(k) \left[G_k(\tau) \hat{a}_{k,\alpha} e^{-i\vec{k} \cdot \vec{x}} + G_k^*(\tau) \hat{a}_{k,\alpha}^\dagger e^{i\vec{k} \cdot \vec{x}} \right], \quad (3.14)$$

where $F_k(\tau)$ and $G_k(\tau)$ obey:

$$F'_k = G_k + \frac{\chi'_E}{\chi_E} F_k, \quad (3.15)$$

$$G'_k = -\frac{k^2}{f} F_k - \frac{\chi'_E}{\chi_E} G_k. \quad (3.16)$$

Equations (3.15)–(3.16) come from Eqs. (3.7)–(3.8) and the mode functions $F_k(\tau)$ and $G_k(\tau)$ must also satisfy the Wronskian normalization condition which follows from the canonical commutators together with the expansions (3.13) and (3.14):

$$F_k(\tau) G_k^*(\tau) - F_k^*(\tau) G_k(\tau) = i. \quad (3.17)$$

The equations for the mode functions can be decoupled with the usual manipulations:

$$F_k'' + \left[\frac{k^2}{f} - \frac{\chi_E''}{\chi_E} \right] F_k = 0, \quad (3.18)$$

$$\overline{G}_k'' + \left[\frac{k^2}{f} - \left(\frac{1}{\chi_B} \right)'' \chi_B \right] \overline{G}_k = 0, \quad (3.19)$$

where $\overline{G}_k = \sqrt{f} G_k$. In terms of F_k and G_k the magnetic and the electric power spectra are⁶

$$P_B(k, \tau) = \frac{k^5}{2 \pi^2 a^4(\tau) f(\tau)} |F_k(\tau)|^2, \quad (3.20)$$

$$P_E(k, \tau) = \frac{k^3}{2 \pi^2 a^4(\tau)} |G_k(\tau)|^2. \quad (3.21)$$

The correlators of the rescaled fields in Fourier space are given by:

$$\langle B_i(\vec{k}, \tau) B_j(\vec{p}, \tau) \rangle = \frac{2\pi^2}{k^3} P_B(k, \tau) P_{ij}(k) \delta^{(3)}(\vec{k} + \vec{p}), \quad (3.22)$$

$$\langle E_i(\vec{k}, \tau) E_j(\vec{p}, \tau) \rangle = \frac{2\pi^2}{k^3} P_E(k, \tau) P_{ij}(k) \delta^{(3)}(\vec{k} + \vec{p}), \quad (3.23)$$

where $P_{ij}(k)$ has been defined after Eq. (3.12) while $B_i(\vec{k}, \tau)$ and $E_i(\vec{k}, \tau)$ are, strictly speaking, field operators in Fourier space but can be also viewed as classical stochastic variables. From Eqs. (3.22)–(3.23) and (2.22) the properly normalized energy density is

$$\rho_E + \rho_B = \int \frac{dk}{k} \left[P_B(k, \tau) + P_E(k, \tau) \right], \quad (3.24)$$

where the 4π factor disappeared because it has been included in the canonical redefinition of the fields.

3.3 Power spectra and duality

Under the duality transformation $\chi_E \rightarrow 1/\chi_B$ and $\chi_B \rightarrow 1/\chi_E$, Eqs. (3.15) and Eq. (3.16) are exchanged provided

$$G_k \rightarrow -\frac{k}{\sqrt{f}} F_k, \quad F_k \rightarrow \frac{\sqrt{f}}{k} G_k, \quad (3.25)$$

⁶The factor $1/f$ in Eq. (3.20) may appear at first sight odd but it comes from the correct relation between the magnetic field and the canonical normal mode \vec{A} .

This property is a consequence of Eq. (3.9) but it can be directly verified. Indeed, using Eq. (3.25), Eq. (3.15) transforms as:

$$F'_k = G_k + \frac{\chi'_E}{\chi_E} F_k \rightarrow \left(\frac{\sqrt{f}}{k} G_k \right)' = -\frac{k}{\sqrt{f}} F_k + \left(\frac{1}{\chi_B} \right)' \chi_B \left(\frac{\sqrt{f}}{k} G_k \right). \quad (3.26)$$

After performing the time derivative on the left-hand side of Eq. (3.26), both sides of the equation can be multiplied by k/\sqrt{f} ; Eq. (3.26) becomes:

$$G'_k = -\frac{k^2}{f} F_k - \left(\frac{\chi'_B}{\chi_B} + \frac{\sqrt{f}'}{\sqrt{f}} \right) G_k, \quad (3.27)$$

which coincides exactly with Eq. (3.16) if we recall that, by definition of f , $\chi_B \sqrt{f} \equiv \chi_E$. Using the transformations of Eq. (3.25), the spectra of Eqs. (3.20) and (3.21) are interchanged, i.e.

$$P_B(k, \tau) \rightarrow P_E(k, \tau), \quad P_E(k, \tau) \rightarrow P_B(k, \tau). \quad (3.28)$$

Equation (3.28) relates different dynamical regimes in the evolution of χ_E and χ_B . In summary, since Eqs. (3.18) and (3.19) are invariant under the generalized duality transformation, also the evolution equations of the mode functions are exchanged by duality. This conclusion implies that the magnetic and electric power spectra are exchanged by the action of the duality symmetry in such a way that the total energy density is left unaltered.

4 Inflationary magnetic and electric power spectra

4.1 General considerations

For an explicit solution of Eqs. (3.18)–(3.19) the susceptibilities shall be parametrized as⁷

$$\chi_E(y) = y^{1/2-\nu}, \quad \chi_B(y) = y^{1/2-\nu+\mu}, \quad f(y) = y^{-2\mu}, \quad (4.1)$$

where $y(\tau) = (-\tau/\tau_i)$ and τ_i marks the initial time of the evolution of the various pump fields and the relevant dynamical evolution occurs for $\tau > -\tau_i$. The parametrization given in Eq. (4.1) is monotonic even if this assumption can be easily relaxed within the same scheme⁸. During the quasi-de Sitter stage of expansion the following standard relations hold between the expansion rates in conformal (i.e. $\mathcal{H} = a'/a$) and in cosmic time (i.e. $H = \dot{a}/a$):

$$\mathcal{H} = aH = -\frac{1}{(1-\epsilon)\tau}, \quad \epsilon = -\frac{\dot{H}}{H^2}, \quad (4.2)$$

⁷Although the variable y can be explicitly expressed either in terms of the conformal time coordinate or in terms of the total number of e-folds elapsed since τ_i (i.e. $\ln y(\tau) = -N_t$), the latter parametrization appears to be more useful than the former when dealing with phenomenological considerations as we shall point out in sec. 5.

⁸ In the case of bouncing models of magnetogenesis the evolution may also be non-monotonic, as argued in the past [24].

where the overdot denotes a derivation with respect to the cosmic time coordinate and ϵ is standard slow-roll parameter. Defining $\alpha = 1/2 - \nu$ and focussing on the case $\mu > 0$ there are three distinct regions in the (α, μ) plane. If $\alpha > 0$, χ_E and χ_B are both decreasing. Conversely, in the region $(\alpha + \mu) > 0$ and $\alpha < 0$ (i.e. $-\mu < \alpha < 0$), χ_E increases while χ_B decreases. Finally χ_E and χ_B are both increasing as a function of τ in the region $\alpha < -\mu < 0$. If $\mu < 0$ (or if the sign of μ is flipped in Eq. (4.1)) the (α, μ) plane is still divided in three regions. More specifically χ_E and χ_B are both decreasing for $0 < \alpha < \mu$. Conversely, in the region $0 < \mu < \alpha$, χ_E decreases while χ_B increases; finally, χ_E and χ_B are both increasing in the region $\alpha < 0$. If we relate $1/\chi_C$ (with $C = B, E$) to the gauge coupling, the increase of χ_C implies a decrease of the gauge coupling and vice versa.

Equation (4.2) holds in the case of conventional inflationary models (see e.g. [25]) where the Universe evolves from strong gravitational coupling to weak gravitational coupling, i.e. the space-time curvature is maximal at the onset of inflation and gets smaller during reheating. It is fair to say that the potential drawbacks of magnetogenesis coincide with the potential drawbacks of conventional models of inflation which are, typically, not geodesically complete in their past history. The considerations reported here can be easily extended to the case of bouncing models (see e.g. [26] for this terminology) evolving from weak gravitational coupling to strong gravitational coupling, i.e. the space-time curvature is small initially and gets larger at the reheating.

The parametrization of Eq. (4.1) is general enough to encompass all the physically interesting cases and the aim of the forthcoming considerations is to relate the electric and magnetic power spectra to the evolution of the susceptibilities. In other words, given a sufficiently general parametrization for the evolution of the susceptibilities such as the one of Eq. (4.1) which are the corresponding power spectra obtainable during a phase of quasi-de Sitter evolution? Are they phenomenologically relevant? These are some of the questions addressed in the present and in the following section.

4.2 Analytic solutions for the mode functions

Inserting Eq. (4.1) into Eqs. (3.18) and (3.19) and defining $z = (-\tau)$, the resulting pair of equations is:

$$F_k'' + \frac{1 - 2p_F}{z} F_k' + \left[\gamma_F^2 q^2 z^{2q-2} + \frac{p_F^2 - \sigma^2 q^2}{z^2} \right] F_k = 0, \quad (4.3)$$

$$\overline{G}_k'' + \frac{1 - 2p_G}{z} \overline{G}_k' + \left[\gamma_G^2 q^2 z^{2q-2} + \frac{p_G^2 - \rho^2 q^2}{z^2} \right] \overline{G}_k = 0, \quad (4.4)$$

where $\overline{G}_k(\tau) = \sqrt{f(\tau)} G_k(\tau)$, and

$$p_F = 1/2, \quad p_G = 1/2, \quad q = (1 + \mu), \quad \gamma_F = \gamma_G = \frac{k}{\tau_i^\mu |1 + \mu|}. \quad (4.5)$$

Equations (4.3) and (4.4) are different from the analog equations obtainable in the case when the susceptibilities are coincident. The solution of Eqs. (4.3)–(4.4) can be obtained in terms of two linear combinations of Bessel functions [27, 28] with indices σ and ρ denoted hereunder by \mathcal{C}_σ and \mathcal{C}_ρ :

$$F_k(z) = z^{p_F} \mathcal{C}_\sigma(\gamma_F z^q), \quad \sigma = \frac{\nu}{1 + \mu}, \quad (4.6)$$

$$\overline{G}_k(z) = z^{p_G} \mathcal{C}_\rho(\gamma_G z^q), \quad \rho = \sigma - 1. \quad (4.7)$$

According to Eq. (3.16), the relation between G_k and F'_k is given by $G_k = F'_k - (\chi'_E/\chi_E)F_k$. Imposing the quantum mechanical normalization, Eqs. (4.6)–(4.7) are expressible in terms of Hankel functions of first kind [27, 28]:

$$F_k(\tau) = \frac{\mathcal{D}}{\sqrt{2k/\sqrt{f(\tau)}}} \sqrt{-k\tau/\sqrt{f(\tau)}} H_\sigma^{(1)}\left(-\frac{k\tau/\sqrt{f(\tau)}}{|1 + \mu|}\right), \quad (4.8)$$

$$G_k(\tau) = -\mathcal{D} \sqrt{\frac{k/\sqrt{f(\tau)}}{2}} \sqrt{-k\tau/\sqrt{f(\tau)}} H_\rho^{(1)}\left(-\frac{k\tau/\sqrt{f(\tau)}}{|1 + \mu|}\right), \quad (4.9)$$

where $|\mathcal{D}|^2 = \pi/(2|1 + \mu|)$; σ and $\rho = \sigma - 1$ have been already defined in Eqs. (4.6)–(4.7). Equations (4.8) and (4.9) satisfy the Wronskian normalization condition of Eq. (3.17). The absolute values $|1 + \mu|$ guarantee that the results are still valid when $\mu \rightarrow -\mu$.

4.3 Explicit form of the power spectra

Inserting Eqs. (4.8)–(4.9) into Eqs. (3.20)–(3.21) the magnetic and the electric power spectra become:

$$P_B(k, \tau, \sigma, \mu) = \frac{H^4}{8\pi|1 + \mu|} \frac{(-k\tau)^5}{f^2(\tau)} \left| H_\sigma^{(1)}\left(\frac{-k\tau/\sqrt{f(\tau)}}{|1 + \mu|}\right) \right|^2, \quad (4.10)$$

$$P_E(k, \tau, \sigma, \mu) = \frac{H^4}{8\pi|1 + \mu|} \frac{(-k\tau)^5}{f^2(\tau)} \left| H_{\sigma-1}^{(1)}\left(\frac{-k\tau/\sqrt{f(\tau)}}{|1 + \mu|}\right) \right|^2. \quad (4.11)$$

Equations (4.10) and (4.11) are exchanged⁹ if $\sigma \rightarrow \tilde{\sigma} = 1 - \sigma$. In terms of the two dimensionless variables $x = -k\tau$ and $y = (-\tau/\tau_i)$, Eqs. (4.10) and (4.11) are

$$P_B(x, y, \sigma, \mu) = \frac{H^4}{8\pi|1 + \mu|} x^5 y^{2\mu} \left| H_\sigma^{(1)}\left(\frac{x y^\mu}{|1 + \mu|}\right) \right|^2, \quad (4.12)$$

$$P_E(x, y, \sigma, \mu) = \frac{H^4}{8\pi|1 + \mu|} x^5 y^{2\mu} \left| H_{\sigma-1}^{(1)}\left(\frac{x y^\mu}{|1 + \mu|}\right) \right|^2. \quad (4.13)$$

⁹For a Hankel function with generic index α and argument z we have that $|H_\alpha^1(z)|^2 = |H_{-\alpha}^1(z)|^2$. Thanks to this property it is possible to show that the electric and magnetic power spectra are exchanged when $\sigma \rightarrow \tilde{\sigma} = 1 - \sigma$. This invariance is related to the duality symmetry.

When the relevant wavelengths are larger than the Hubble radius it is practical to introduce yet another variable defined as $w = x y^\mu$. In the (y, w) plane, Eqs. (4.12) and (4.13) read:

$$P_B(y, w, \sigma, \mu) = \frac{H^4}{8\pi |1 + \mu|} w^5 y^{-3\mu} \left| H_\sigma^{(1)} \left(\frac{w}{|1 + \mu|} \right) \right|^2, \quad (4.14)$$

$$P_E(y, w, \sigma, \mu) = \frac{H^4}{8\pi |1 + \mu|} w^5 y^{-3\mu} \left| H_{\sigma-1}^{(1)} \left(\frac{w}{|1 + \mu|} \right) \right|^2. \quad (4.15)$$

Wavelengths larger than the Hubble radius correspond to the condition $|k/\sqrt{f}| < \mathcal{H}$. The case $\mu = -1$ is singular since, in this case, k^2/f and χ_E''/χ_E evolve roughly at the same rate. This implies that the modes that are larger than the Hubble rate at τ_i will never reenter while the modes inside the Hubble radius at τ_i will never exit. In the limit $w \ll 1$ the corresponding wavelengths are larger than the Hubble radius and the power spectra of Eqs. (4.14)–(4.15) become

$$P_B(x, y, \sigma) = H^4 \mathcal{Q}_B(\sigma, \mu) x^{5-2|\sigma|} y^{-2\mu(|\sigma|-1)}, \quad (4.16)$$

$$P_E(x, y, \sigma) = H^4 \mathcal{Q}_E(\sigma, \mu) x^{5-2|\sigma-1|} y^{-2\mu(|\sigma-1|-1)}, \quad (4.17)$$

where

$$\begin{aligned} \mathcal{Q}_B(\sigma, \mu) &= \frac{\Gamma^2(|\sigma|)}{\pi^3} 2^{2|\sigma|-3} |1 + \mu|^{2|\sigma|-1}, \\ \mathcal{Q}_E(\sigma, \mu) &= \frac{\Gamma^2(|\sigma-1|)}{\pi^3} 2^{2|\sigma-1|-3} |1 + \mu|^{2|\sigma-1|-1}. \end{aligned} \quad (4.18)$$

The amplitude of the spectra of Eqs. (4.16)–(4.17) depends on σ and on μ : on the one hand σ is defined in terms of μ and ν (i.e. $\sigma = \nu/(1 + \mu)$), on the other hand μ controls the overall suppression or enhancement of the spectrum through the y -dependent prefactor that is related to the total number of efolds. To proceed further a more transparent parametrization of the spectral indices is desirable.

4.4 Spectral indices

The magnetic and the electric spectral indices are defined as:

$$n_B - 1 = \frac{\partial P_B(x, y, \sigma, \mu)}{\partial \ln x}, \quad n_E - 1 = \frac{\partial P_E(x, y, \sigma, \mu)}{\partial \ln x}, \quad (4.19)$$

where the scale-invariant limits correspond to $n_E \rightarrow 1$ and $n_B \rightarrow 1$. The power spectrum of curvature perturbations $\mathcal{P}_{\mathcal{R}}(k)$ is assigned (see e.g. [29, 30, 31]) within the same conventions

$$\mathcal{P}_{\mathcal{R}}(k) = \mathcal{A}_{\mathcal{R}} \left(\frac{k}{k_p} \right)^{n_s-1}, \quad k_p = 0.002 \text{ Mpc}^{-1}, \quad (4.20)$$

where $\mathcal{A}_{\mathcal{R}}$ (the spectral amplitude at the pivot scale k_p) determines the inflationary rate of expansion and enters directly the amplitude of the magnetic and electric power spectra (see

sec. 5); n_s is the scalar spectral index. As implied by the absolute values appearing in Eqs. (4.16)–(4.17), the power spectra have three different analytic forms depending on the values of σ :

- if $\sigma > 1$ the magnetic and the electric spectral indices are, respectively $n_B = 6 - 2\sigma$ and $n_E = 8 - 2\sigma$; the consistency between the two indices implies, in this region, $n_E = n_B + 2$;
- if $0 < \sigma < 1$ the slope of the electric power spectrum is unchanged in comparison with the previous case; on the contrary n_E is given by $n_E = 4 + 2\sigma$; the consistency between n_E and n_B implies, in this case, $n_E = 10 - n_B$;
- if $\sigma < 0$ the magnetic and the electric spectral indices are, respectively, $n_B = 6 + 2\sigma$ and $n_E = 4 + 2\sigma$, implying $n_E = n_B - 2$.

Consider now the limit $\mu \rightarrow 0$ (see also Eq. (2.32)): when $\mu \rightarrow 0$, $f \rightarrow 1$, $\chi_E = \chi_B = \sqrt{\lambda}$ and $\sigma \rightarrow \nu$. All the relations between the spectral indices and σ deduced in the previous list remain true in the limit $\mu \rightarrow 0$ provided σ is replaced by ν . When $\mu \neq 0$ the spectral indices and the corresponding amplitudes are determined by not only by ν but also by μ : what was a line in the parameter space connecting n_B (or n_E) to ν becomes now a plane. This is, in a nutshell, the rationale for the widening of the parameter space of the model.

4.5 Regions in the parameter space

Although the parameter space of the model can be charted either in the (μ, ν) plane or in the (μ, σ) plane, the latter parametrization turns out to be more useful than the former since the spectral indices have a simpler dependence in terms of σ . Moreover since $\nu = \sigma(1 + \mu)$, ν can be eliminated from the rate of variation of the susceptibilities of Eq. (4.1) so that $\ln \chi_E = [1/2 - \sigma(1 + \mu)] \ln y$ and $\ln \chi_B = [1/2 + \mu - \sigma(1 + \mu)] \ln y$. From these expressions we can say that χ_E and χ_B are both decreasing during the quasi-de Sitter stage of expansion provided $[1/2 - \sigma(1 + \mu)] > 0$ and $[1/2 + \mu - \sigma(1 + \mu)] > 0$. With similar logic the entire parameter space can be discussed. In Fig. 1 the various regions of the (σ, μ) plane are reported. Below the two *dashed* branches of hyperbola χ_B is decreasing. Similarly, below the two *full* branches of hyperbola χ_E is decreasing. Above the same curves (either dashed or full) the situation is reversed and the corresponding susceptibilities increase rather than decreasing.

The shaded area of Fig. 1 (bounded from above by the dashed hyperbola and from below by the full hyperbola) describes an intermediate situation: in this region χ_B decreases while χ_E increases. In Fig. 1 the two horizontal dotted lines are the asymptotes of the two hyperbolae (i.e. $\sigma = 0$ and $\sigma = 1$) but they are also the boundaries of the three regions characterizing the different values of the spectral indices discussed in the list of items of the previous subsection. The line $\mu = -1$ (i.e. the common vertical asymptote of

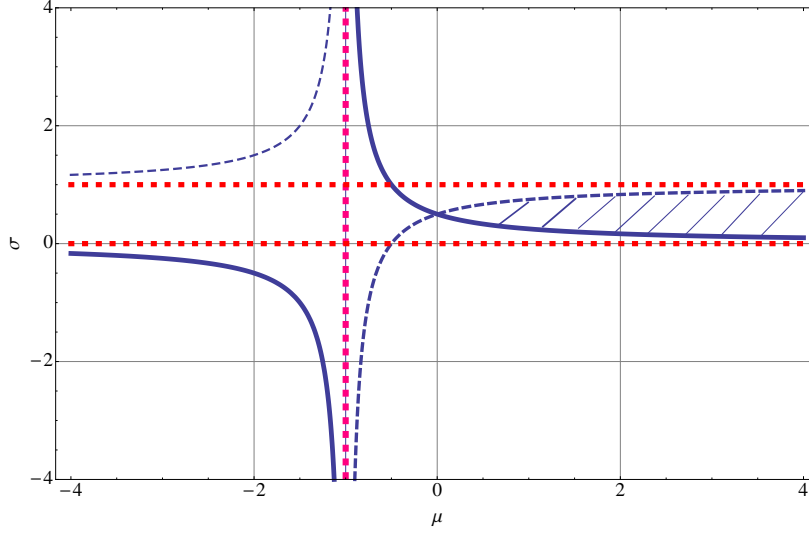


Figure 1: The regions of the (σ, μ) plane are illustrated.

both hyperbolae) has been already discussed after Eqs. (4.14)–(4.15): when $\mu = -1$ the pumping action due to the susceptibility and to the refractive index are exactly balanced (i.e. $1/f \simeq \chi_E''/\chi_E$) and both proportional to τ^{-2} .

5 Phenomenology

5.1 Power spectra in critical units

From Eq. (3.24) the electric and magnetic energy densities in critical units are:

$$\Omega_B(x, y, \sigma, \mu) = \frac{8\pi}{3} \frac{P_B(x, y, \sigma, \mu)}{H^2 M_P^2}, \quad \Omega_E(x, y, \sigma, \mu) = \frac{8\pi}{3} \frac{P_E(x, y, \sigma, \mu)}{H^2 M_P^2}, \quad (5.1)$$

where M_P is the Planck mass. Inserting Eqs. (4.16) and (4.17) into Eq. (5.1) and recalling the notations of Eqs. (4.2) and (4.20), Eq. (5.1) leads to the following pair of equations:

$$\Omega_B(x, y, \sigma, \mu) = \frac{8\pi^2}{3} \epsilon \mathcal{A}_{\mathcal{R}} \mathcal{Q}_B(\sigma, \mu) x^{5-2|\sigma|} y^{-2\mu(|\sigma|-1)}, \quad (5.2)$$

$$\Omega_E(x, y, \sigma, \mu) = \frac{8\pi^2}{3} \epsilon \mathcal{A}_{\mathcal{R}} \mathcal{Q}_E(\sigma, \mu) x^{5-2|\sigma-1|} y^{-2\mu(|\sigma-1|-1)}. \quad (5.3)$$

In Eqs. (5.2)–(5.3) the inflationary Hubble rate has been expressed in terms of the amplitude of adiabatic curvature perturbations. The fiducial set of cosmological parameters¹⁰ used

¹⁰Using the standard terminology Ω_{b0} , Ω_{c0} and Ω_{de0} are the critical fractions of baryons, dark matter and dark energy; h_0 is the Hubble rate at the present time and in units of 100 km/sec Mpc; n_s and ϵ_{re} are, respectively, the spectral index of curvature perturbations and the optical depth at reionization.

hereunder comes from the comparison of the concordance paradigm with the WMAP 9 yr data alone [29] (see also [30, 31]):

$$(\Omega_{b0}, \Omega_{c0}, \Omega_{de0}, h_0, n_s, \epsilon_{re}) \equiv (0.0463, 0.233, 0.721, 0.700, 0.972, 0.089), \quad (5.4)$$

with $\mathcal{A}_{\mathcal{R}} = 2.41 \times 10^{-9}$. The combinations of other data sets lead to slight differences in the pivotal parameters but these differences have no relevance in the present context. For instance, using the data of the baryon acoustic oscillations (see, e.g. [32]) in combination with the WMAP 9 yr data, the six parameters of Eq. (5.4) are modified at the level of the few percent and $\mathcal{A}_{\mathcal{R}} = 2.35 \times 10^{-9}$. Another set of concordance parameters is obtained by combining the WMAP 9 yr data with the direct determinations of the Hubble rate giving $\mathcal{A}_{\mathcal{R}} = 2.45 \times 10^{-9}$. The differences in the values of $\mathcal{A}_{\mathcal{R}}$ are immaterial for the present considerations. The same comment holds for the values of ϵ whose upper limits range from $\epsilon < 0.023$ in the case of WMAP 9 yr data alone to $\epsilon < 0.0081$ when the WMAP 9 yr data are combined with all the other data (see e.g. [32, 33, 34, 35, 36, 37, 38]). The Planck explorer data, at least in their current release, do not lead to crucial differences in the determinations of the concordance parameters and cannot be used alone but must be combined, in some way, with the WMAP data.

5.2 Dependence on the number of efolds

The variable x appearing in Eqs. (5.1), (5.2) and (5.3) can be expressed as:

$$x = \frac{k}{(1-\epsilon)aH} = \frac{k}{H_0} e^{-N_{\max}} \left[1 + \epsilon + \mathcal{O}(\epsilon^2) \right] \quad (5.5)$$

$$\simeq 6.35 \times 10^{-24} \left(\frac{k}{\text{Mpc}^{-1}} \right) \left(\frac{h_0}{0.7} \right)^{-1} \left(\frac{\epsilon}{0.01} \right)^{-1/4} \left(\frac{\mathcal{A}_{\mathcal{R}}}{2.41 \times 10^{-9}} \right)^{-1/4}, \quad (5.6)$$

where $H_0 = 100 h_0 \text{ Mpc}^{-1} \text{ km/sec}$ is the present value of the Hubble rate and N_{\max} is the maximal number of efolds which are today accessible to our observations [39]. In practice N_{\max} is determined by fitting the redshifted inflationary event horizon inside the present Hubble radius H_0^{-1} :

$$e^{N_{\max}} = (2\pi\epsilon\mathcal{A}_{\mathcal{R}}\Omega_{R0})^{1/4} \left(\frac{M_P}{H_0} \right)^{1/2} \left(\frac{H_r}{H} \right)^{\gamma-1/2}, \quad (5.7)$$

where Ω_{R0} is the present critical fraction of radiation (in the concordance model $h_0^2\Omega_{R0} = 4.15 \times 10^{-5}$). From Eq. (5.4) and in the sudden reheating approximation we have $N_{\max} \simeq 63.25 + 0.25 \ln \epsilon$ which is numerically close to the minimal number of efolds N_{\min} needed to solve the kinematic problems of the standard cosmological model (i.e. $N_{\min} \simeq N_{\max}$).

Because of the possibility of a delayed reheating the value of N_{\max} suffers of a certain degree of theoretical uncertainty which can be roughly quantified in 15 efolds. Indeed, Eq. (5.7) assumes that the reheating is concluded at a typical scale $H_r \geq 10^{-44} M_P$ i.e. just

prior to the formation of the light nuclei. The expansion rate during the intermediate phase between H and H_r is controlled by γ which can be either smaller than $1/2$ or larger than $1/2$; the case $\gamma = 1/2$ corresponds to the sudden reheating approximation when the intermediate phase is absent from Eq. (5.7). If $\gamma - 1/2 > 0$ (as it happens if $\gamma = 2/3$ when the post-inflationary background is dominated by dust) N_{\max} diminishes in comparison with the case when $H = H_r$. Conversely, if $\gamma - 1/2 < 0$ (as it happens if $\gamma = 1/3$ when the post-inflationary background is dominated by stiff sources), N_{\max} increases. The maximal increase (of about 15 efolds) occurs when the post-inflationary evolution is dominated by stiff sources down to the epoch of formation of light nuclei. Moreover, defining N_t as the total number of efolds elapsed since τ_i , if $N_t > N_{\max}$, the redshifted value of the inflationary event horizon is larger than the present value of the Hubble radius.

To summarize the previous considerations, the pivot values considered in the numerical examples will be $N_{\max} = 63.25 + 0.25 \ln \epsilon$ and $N_t = 80$. These values are both conservative and illustrative given the unavoidable uncertainty about the total duration of the inflationary phase and, to some extent, on the post-inflationary expansion rate.

5.3 Post-inflationary evolution

For the standard thermal history with sudden reheating, the conductivity σ_c jumps at a finite value at the end of inflation and the continuity of the electric and magnetic fields implies that the amplitude of the electric power spectrum gets suppressed, at a fixed time, as $(k/\sigma_c)^2$ in comparison with its magnetic counterpart [12]. Both power spectra are exponentially suppressed, for sufficiently large k , as $\exp[-2(k^2/k_\sigma^2)]$ where $k_\sigma^{-2} = \int_{\tau_\sigma}^{\tau} d\tau' / [4\pi\sigma_c(\tau')]$. The evaluation of k_σ is complicated by the fact that the integral extends well after τ_σ . This estimate can be made rather accurate by computing the transport coefficients of the plasma in different regimes [40]. By taking $\tau = \tau_{\text{eq}}$ the following approximate expression holds:

$$\left(\frac{k}{k_\sigma}\right)^2 \simeq \frac{10^{-26}}{\sqrt{2 h_0^2 \Omega_{\text{M}0} (z_{\text{eq}} + 1)}} \left(\frac{k}{\text{Mpc}^{-1}}\right)^2, \quad (5.8)$$

where $\Omega_{\text{M}0} = \Omega_{\text{c}0} + \Omega_{\text{b}0}$ and $z_{\text{eq}} \simeq 3200$. Eq. (5.8) shows that $\exp[-2(k/k_\sigma)^2]$ is so close to 1 to give negligible suppression for $\mathcal{O}(10^{-4} \text{Mpc}^{-1}) \leq k \leq \mathcal{O}(\text{Mpc}^{-1})$ where the magnetogenesis considerations apply. The effect of the conductivity is particularly important for blue (i.e. $n_B \geq 1$) or violet (i.e. $n_B \gg 1$) power spectra since, in these cases, the back-reaction bounds are more constraining at small scales (i.e. large k -modes). Equation (5.8) would imply that $k_\sigma \simeq 10^{13} \text{Mpc}^{-1}$ but, to be on the safe side, we shall be even more demanding and require, in the case of increasing power spectra, the back-reaction constraints are met at an even smaller length-scale which is the one corresponding to $x \simeq 1$, i.e. $k \sim aH$.

In summary we can say that there are two different physical situations:

- the case of blue or violet spectra (i.e. $n_B > 1$): in this case the most relevant constraint come from the scales affected by the conductivity; to be conservative the constraints

shall be applied for $k \sim aH$ even if over these scales the power spectra are exponentially suppressed;

- the case of red spectra (i.e. $n_B < 1$) in this case the most relevant constraints come from large wavelengths or, in equivalent terms, from small wavenumbers in the range $10^{-4} \text{ Mpc}^{-1} \leq k \leq \text{Mpc}^{-1}$.

5.4 The case $\sigma > 1$

Inserting Eqs. (4.16)–(4.17) into Eqs. (5.2)–(5.3), the explicit form of the power spectra for $\sigma > 1$ is:

$$\Omega_B(k, N_t, \sigma, \mu) = \frac{8\pi^2}{3} \mathcal{A}_{\mathcal{R}} \epsilon \mathcal{Q}_B(\sigma, \mu) \left(\frac{k}{aH} \right)^{5-2\sigma} e^{2\mu N_t(\sigma-1)}, \quad (5.9)$$

$$\Omega_E(k, N_t, \sigma, \mu) = \frac{8\pi^2}{3} \mathcal{A}_{\mathcal{R}} \epsilon \mathcal{Q}_E(\sigma, \mu) \left(\frac{k}{aH} \right)^{7-2\sigma} e^{2\mu N_t(\sigma-2)}. \quad (5.10)$$

Using Eq. (4.19) into Eqs. (5.9) and (5.10), the magnetic and electric spectral indices are, respectively, $n_B = 6 - 2\sigma$ and $n_E = 8 - 2\sigma$; moreover, since $\sigma > 1$ the magnetic spectral index is bounded from above, i.e. $n_B < 4$. Eliminating σ between the explicit expressions of n_B and n_E , the power spectra of Eqs. (5.9) and (5.10) are phrased in terms of n_B and μ :

$$\Omega_B(k, N_t, n_B, \mu) = \frac{8\pi^2}{3} \mathcal{A}_{\mathcal{R}} \epsilon \mathcal{Q}_B(n_B, \mu) \left(\frac{k}{aH} \right)^{n_B-1} e^{\mu N_t(4-n_B)}, \quad (5.11)$$

$$\Omega_E(k, N_t, n_B, \mu) = \frac{8\pi^2}{3} \mathcal{A}_{\mathcal{R}} \epsilon \mathcal{Q}_E(n_B, \mu) \left(\frac{k}{aH} \right)^{n_B+1} e^{\mu N_t(2-n_B)}, \quad (5.12)$$

where the prefactors $\mathcal{Q}_B(n_B, \mu)$ and $\mathcal{Q}_E(n_B, \mu)$ are, in this case:

$$\mathcal{Q}_B(n_B, \mu) = \frac{2^{3-n_B}}{\pi^3} \Gamma^2\left(\frac{6-n_B}{2}\right) |1+\mu|^{5-n_B}, \quad \frac{\mathcal{Q}_B(n_B, \mu)}{\mathcal{Q}_E(n_B, \mu)} = (4-n_B)^2 |1+\mu|^2. \quad (5.13)$$

If $n_B \rightarrow 1$ in Eqs. (5.11) and (5.12) the magnetic power spectrum is scale-invariant while the electric power spectrum is blue, i.e.

$$\Omega_B(k, N_t, 1, \mu) = \frac{8\pi^2}{3} \mathcal{A}_{\mathcal{R}} \epsilon \mathcal{Q}_B(1, \mu) e^{3\mu N_t}, \quad (5.14)$$

$$\Omega_E(k, N_t, 1, \mu) = \frac{8\pi^2}{3} \mathcal{A}_{\mathcal{R}} \epsilon \mathcal{Q}_E(1, \mu) \left(\frac{k}{aH} \right)^2 e^{\mu N_t}. \quad (5.15)$$

If $n_B \rightarrow -1$ the electric power spectrum is scale-invariant while the magnetic power spectrum is sharply red:

$$\Omega_B(k, N_t, -1, \mu) = \frac{8\pi^2}{3} \mathcal{A}_{\mathcal{R}} \epsilon \mathcal{Q}_B(-1, \mu) \left(\frac{k}{aH} \right)^{-2} e^{5\mu N_t}, \quad (5.16)$$

$$\Omega_E(k, N_t, -1, \mu) = \frac{8\pi^2}{3} \mathcal{A}_{\mathcal{R}} \epsilon \mathcal{Q}_E(-1, \mu) e^{3\mu N_t}. \quad (5.17)$$

Recalling Eq. (4.6), the relation among σ , μ and ν is given by $\sigma = \nu/(1+\mu)$. Consequently, in the limit $\mu \rightarrow 0$ and $n_B \sim 1$ we also have $\sigma = \nu = 5/2$. In the latter case the magnetic power spectrum at the time of gravitational collapse can be estimated as¹¹ $\sqrt{P_B} \simeq \mathcal{O}(0.01 \text{ nG})$. This is the result found in [9, 12, 22] and it is compatible with the origin of large-scale magnetic fields.

The magnetogenesis requirements [4, 9, 12, 22] roughly demand that the magnetic fields at the time of the gravitational collapse of the protogalaxy should be approximately larger than a (minimal) field which can be estimated between 10^{-16} nG and 10^{-11} nG . The most optimistic estimate is derived by assuming that every rotation of the galaxy would increase the magnetic field of one efold. The number of galactic rotations since the collapse of the protogalaxy can be estimated between 30 and 35, leading approximately to a purported growth of 13 orders of magnitude. During collapse of the protogalaxy compressional amplification will increase the field of about 5 orders of magnitude. Thus the required seed field at the onset of the gravitational collapse must be, at least, as large as 10^{-15} nG or, more realistically, larger than 10^{-11} nG [9, 22]. For $\sigma > 1$, $\mathcal{A}_R = 2.41 \times 10^{-9}$ and $\epsilon = 0.01$ the magnetic power spectrum at the onset of the gravitational collapse of the protogalaxy can be written as:

$$\frac{P_B(k, N_t, n_B, \mu)}{G^2} = 10^{-21.05} \left(\frac{k}{H_0} \right)^{n_B-1} e^{-(n_B-1)N_{\max}} e^{\mu N_t(4-n_B)}. \quad (5.18)$$

Consider now the case when both spectra are strongly increasing or, as we say for short, violet. For instance, if $n_B = 3$ the magnetic and the electric spectra are given, respectively, by:

$$\Omega_B(k, N_t, 3, \mu) = \frac{8\pi^2}{3} \mathcal{A}_R \epsilon \mathcal{Q}_B(3, \mu) \left(\frac{k}{aH} \right)^2 e^{\mu N_t}, \quad (5.19)$$

$$\Omega_E(k, N_t, 3, \mu) = \frac{8\pi^2}{3} \mathcal{A}_R \epsilon \mathcal{Q}_E(3, \mu) \left(\frac{k}{aH} \right)^4 e^{-\mu N_t}. \quad (5.20)$$

The constraints on the violet and blue spectra are imposed at $x \simeq 1$; these scales are actually washed out by the finite value of the conductivity and, in this sense, this requirement is rather conservative. The requirements $\Omega_B(aH, N_t, 3, \mu) < 10^{-3}$ and $\Omega_E(aH, N_t, 3, \mu) < 10^{-3}$ cannot be jointly satisfied for $n_B = 3$ as it is clear from Eqs. (5.19)–(5.20). The same conclusion holding for $n_B = 3$ can be extended to the case $n \geq 2$; from Eqs. (5.11)–(5.12) the following conditions can be derived for $k \simeq aH$:

$$\Omega_B(aH, N_t, n_B, \mu) = \frac{8\pi^2}{3} \mathcal{A}_R \epsilon \mathcal{Q}_B(n_B, \mu) e^{\mu N_t(4-n_B)} < 10^{-3}, \quad (5.21)$$

$$\Omega_E(aH, N_t, n_B, \mu) = \frac{8\pi^2}{3} \mathcal{A}_R \epsilon \mathcal{Q}_E(n_B, \mu) e^{\mu N_t(2-n_B)} < 10^{-3}, \quad (5.22)$$

cannot be jointly satisfied. The conditions imposed by Eqs. (5.21)–(5.22) can be relaxed if the maximal wavenumber is not given by $x \sim 1$ but rather by $x_\sigma = k_\sigma/(aH) \simeq 10^{-13}$. In the

¹¹We express the fields in Gauss and $1 \text{ nG} = 10^{-9} \text{ G}$.

latter case larger spectral indices $n_B \geq 2$ can be accommodated and the parameter space may get even wider. In what follows this potentially interesting aspect shall be neglected.

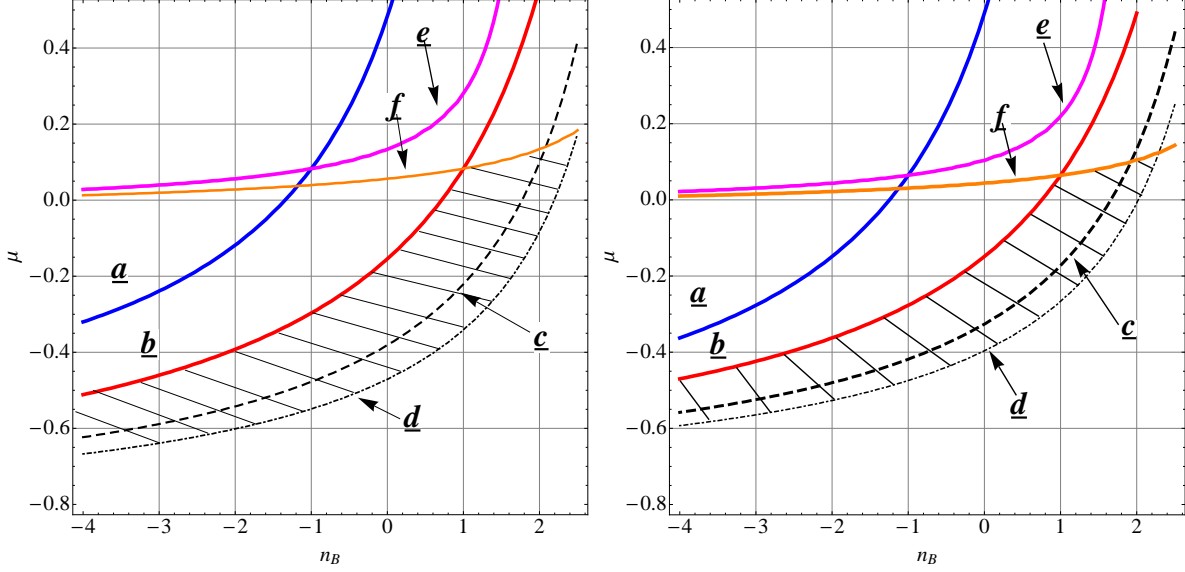


Figure 2: The various constraints of the case $\sigma > 1$ are illustrated. The shaded area represents the allowed region in the parameter space where the back-reaction constraints are avoided and the minimal magnetogenesis requirements satisfied.

Recalling Eq. (5.5), Eqs. (5.9)–(5.10) can be directly expressed in terms of N_{\max} and N_t :

$$\Omega_B(k, N_t, n_B, \mu) = \frac{8\pi^2}{3} \mathcal{A}_{\mathcal{R}} \in \mathcal{Q}_B(n_B, \mu) \left(\frac{k}{H_0} \right)^{n_B-1} e^{\mathcal{F}_B(\mu, N_t, n_B)}, \quad (5.23)$$

$$\Omega_E(k, N_t, n_B, \mu) = \frac{8\pi^2}{3} \mathcal{A}_{\mathcal{R}} \in \mathcal{Q}_E(n_B, \mu) \left(\frac{k}{H_0} \right)^{n_B+1} e^{\mathcal{F}_E(\mu, N_t, n_B)}. \quad (5.24)$$

where

$$\begin{aligned} \mathcal{F}_B(\mu, N_t, N_{\max}, n_B) &= -N_{\max}(n_B - 1) + \mu N_t(4 - n_B), \\ \mathcal{F}_E(\mu, N_t, N_{\max}, n_B) &= -N_{\max}(n_B + 1) + \mu N_t(2 - n_B). \end{aligned} \quad (5.25)$$

In Fig. 2, for two illustrative choices of the parameters, we plot six different contours corresponding to the curves labeled by (a), (b), (c), (d), (e) and (f):

- the curves (a) and (b) correspond, respectively, to $\Omega_E(k, N_t, n_B, \mu) = 10^{-3}$ and $\Omega_B(k, N_t, n_B, \mu) = 10^{-3}$ when $k = 1 \text{ Mpc}^{-1}$ and $N_t = N_{\max}$ (plot on the left) and when $k = 10^{-4} \text{ Mpc}^{-1}$ and $N_t = 80 > N_{\max}$ (plot on the right); these low-frequency bounds are the most constraining for red spectra;
- the curves (c) and (d) correspond, respectively, to $P_B(k, N_t, n_B, \mu) = 10^{-22} \text{ nG}^2$ and to $P_B(k, N_t, n_B, \mu) = 10^{-32} \text{ nG}^2$; the parameters of the plots are $k = 1 \text{ Mpc}^{-1}$ (roughly

corresponding to the scale of protogalactic collapse) for both plots; moreover the total number of e-folds is such that $N_t = N_{\max}$ (plot on the left) and $N_t = 80 > N_{\max}$ (plot on the right);

- the curves (f) and (e) illustrate, respectively, the contours of Eqs. (5.21) and (5.22) for $N_t = N_{\max}$ (plot on the left) and for $k = 10^{-4} \text{ Mpc}^{-1}$ and $N_t = 80 > N_{\max}$ (plot on the right); these requirements are the most constraining for blue and violet spectra;
- the shaded area is the allowed region in the parameter space where the back reaction constraints are safely enforced and the magnetogenesis requirements are met.

Note that when N_t increases beyond N_{\max} the area of the allowed region gets narrower.

The shaded area of Fig. 2 can be compared with Fig. 1. For $\sigma > 1$ the relation to the magnetic power spectrum is given by $\sigma = (6 - n_B)/2$. The conditions implied by Fig. 1 demand that χ_E and χ_B are both decreasing provided the two following inequalities are simultaneously satisfied:

$$n_B \geq \frac{6\mu + 5}{\mu + 1}, \quad n_B \geq \frac{4\mu + 5}{\mu + 1}, \quad (5.26)$$

where the first inequality refers to χ_E while the second inequality refers to χ_B . Since n_B is bounded from above (i.e. $n_B < 4$ because $\sigma > 1$) it follows that for $\mu < -1$ the first inequality of Eq. (5.26) is never satisfied while the second may or may not be satisfied. Thus, for $\mu < -1$ and $n_B < 4$, χ_E must necessarily increase while χ_B may either increase or decrease.

If $\mu > -1$ the second inequality of Eq. (5.26) is always verified since $n_B \rightarrow 4$ is the asymptote of the corresponding hyperbola. The first inequality may or may not be satisfied. Moreover, since the line $n_B = 4$ intersects the hyperbola, μ will be bounded from below by the asymptote and from above by the intersection; we will then have that the relevant range is $-1 < \mu \leq -1/2$. We can then say that for $-1 < \mu \leq -1/2$ and $n_B < 4$ the magnetic susceptibility χ_B is always decreasing while χ_E may either increase or decrease.

So we can conclude by saying that magnetogenesis is viable and the back reaction constraints safely satisfied in the regions illustrated in Fig. 3. The models are dynamically realized in a number of ways but, in this case (i.e. $\sigma > 1$) *at least one of the susceptibilities must be increasing*.

5.5 The case $0 < \sigma < 1$

In the remaining two regions of the parameter space the analysis follows the same steps already outlined in the case $\sigma > 1$. The logic of the discussion will be exactly the same so that we shall skip the details and stick to the results. If $0 < \sigma < 1$ the power spectra of Eqs. (5.2) and (5.3) become:

$$\Omega_B(k, N, \sigma, \mu) = \frac{8\pi^2}{3} \mathcal{A}_{\mathcal{R}} \epsilon \mathcal{Q}_B(\sigma, \mu) \left(\frac{k}{aH} \right)^{5-2\sigma} e^{2\mu N_t(\sigma-1)}, \quad (5.27)$$

$$\Omega_E(k, N, \sigma, \mu) = \frac{8\pi^2}{3} \mathcal{A}_{\mathcal{R}} \epsilon \mathcal{Q}_E(\sigma, \mu) \left(\frac{k}{aH}\right)^{3+2\sigma} e^{-2\mu N_t \sigma}. \quad (5.28)$$

From Eq. (5.27) σ can be expressed in terms of the magnetic spectral index n_B as $\sigma =$

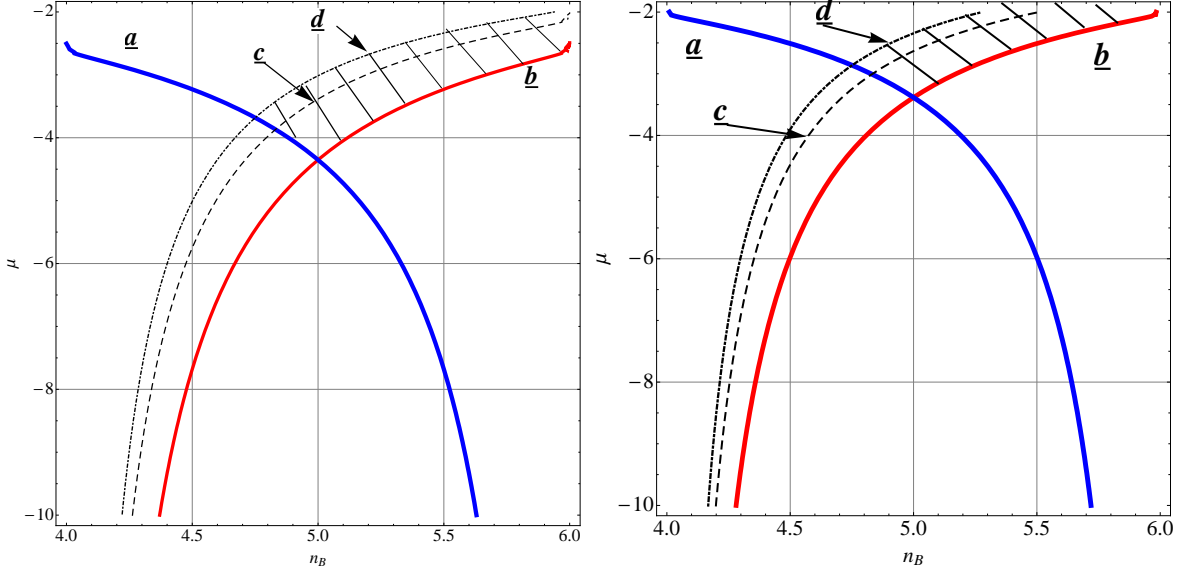


Figure 3: The exclusion plot in the case $0 < \sigma < 1$. The shaded area illustrates the region where the magnetogenesis requirements and the large-scale back-reaction constraints are satisfied. Since, in this case, the spectra are always violet the most significant constraints arise from the maximally amplified length-scale. These constraints cannot be jointly satisfied within the shaded area of this plot so that magnetogenesis is not viable in this case.

$(6 - n_B)/2$. However, since $0 < \sigma < 1$ we must also demand, this time, that $4 < n_B < 6$. In terms of n_B Eqs. (5.27) and (5.28) can be written as:

$$\Omega_B(k, N_t, n_B, \mu) = \frac{8\pi^2}{3} \mathcal{A}_{\mathcal{R}} \epsilon \mathcal{Q}_B(n_B, \mu) \left(\frac{k}{aH}\right)^{n_B-1} e^{\mu N_t(4-n_B)}, \quad (5.29)$$

$$\Omega_E(k, N_t, n_B, \mu) = \frac{8\pi^2}{3} \mathcal{A}_{\mathcal{R}} \epsilon \mathcal{Q}_E(n_B, \mu) \left(\frac{k}{aH}\right)^{9-n_B} e^{-\mu N_t(6-n_B)}, \quad (5.30)$$

where, in this case,

$$\begin{aligned} \mathcal{Q}_B(n_B, \mu) &= \frac{2^{3-n_B}}{\pi^3} \Gamma^2\left(\frac{6-n_B}{2}\right) |1 + \mu|^{5-n_B}, \\ \mathcal{Q}_E(n_B, \mu) &= \frac{2^{n_B-7}}{\pi^3} \Gamma^2\left(\frac{n_B-4}{2}\right) |1 + \mu|^{n_B-5}. \end{aligned} \quad (5.31)$$

In the range $4 < n_B < 6$ the scale-invariant magnetic power spectrum and the scale-invariant electric power spectrum are both impossible since the corresponding values of n_B are located outside the interval.

In Fig. 3 the conditions $\Omega_E(k, N_t, n_B, \mu) = 10^{-3}$ and $\Omega_B(k, N_t, n_B, \mu) = 10^{-3}$ correspond, respectively, to the curves (a) and (b) where $k = 1 \text{ Mpc}^{-1}$ and $N_t = N_{\text{max}}$ (plot on the left); similarly in the plot on the right $k = 10^{-4} \text{ Mpc}^{-1}$ and $N_t = 80$. The curves (c) and (d) denote the same magnetogenesis requirements of Fig. 2 but illustrated in terms of the power spectra (5.29) and (5.30). The shaded area is the region where the (large-scale) back-reaction constraints and the magnetogenesis bounds are jointly satisfied. In spite of that the shaded area must be excluded. Indeed, as it is clear from Eqs. (5.29) and (5.30), for $4 < n_B < 6$ both electric and magnetic spectra are violet. Hence the most significant constraints will come from the region $x \sim 1$ (or $k \sim aH$). Setting $k \sim aH$ in Eqs. (5.29) and (5.30)

$$\Omega_B(k, N_t, n_B, \mu) = \frac{8\pi^2}{3} \mathcal{A}_{\mathcal{R}} \in \mathcal{Q}_B(n_B, \mu) e^{\mu N_t(4-n_B)} < 10^{-3}, \quad (5.32)$$

$$\Omega_E(k, N_t, n_B, \mu) = \frac{8\pi^2}{3} \mathcal{A}_{\mathcal{R}} \in \mathcal{Q}_E(n_B, \mu) e^{-\mu N_t(6-n_B)} < 10^{-3}. \quad (5.33)$$

These conditions are jointly verified, as it can be easily checked, provided the values of μ are well *above* the shaded area of Fig. 3. Since no overlaps between the regions exists there are no viable models of magnetogenesis when $0 < \sigma < 1$.

5.6 The case $\sigma < 0$

Inserting Eqs. (4.16)–(4.17) into Eqs. (5.2)–(5.3), the explicit form of the power spectra in the case $\sigma < 0$ is:

$$\Omega_B(k, N_t, \sigma, \mu) = \frac{8\pi^2}{3} \mathcal{A}_{\mathcal{R}} \in \mathcal{Q}_B(\sigma, \mu) \left(\frac{k}{aH}\right)^{5+2\sigma} e^{-2\mu N_t(\sigma+1)}, \quad (5.34)$$

$$\Omega_E(k, N_t, \sigma, \mu) = \frac{8\pi^2}{3} \mathcal{A}_{\mathcal{R}} \in \mathcal{Q}_E(\sigma, \mu) \left(\frac{k}{aH}\right)^{3+2\sigma} e^{-2\mu N_t\sigma}. \quad (5.35)$$

According to Eqs. (5.34) and (5.35) and using Eq. (4.19) the magnetic and electric spectral indices are, respectively, $n_B = 6 + 2\sigma$ and $n_E = 4 + 2\sigma$. Since $\sigma = (n_B - 6)/2$, the condition $\sigma < 0$ implies $n_B < 6$. Eliminating σ in favour of n_B , Eqs. (5.34) and (5.35) become

$$\Omega_B(k, N_t, n_B, \mu) = \frac{8\pi^2}{3} \mathcal{A}_{\mathcal{R}} \in \mathcal{Q}_B(n_B, \mu) \left(\frac{k}{aH}\right)^{n_B-1} e^{-\mu N_t(n_B-4)}, \quad (5.36)$$

$$\Omega_E(k, N_t, n_B, \mu) = \frac{8\pi^2}{3} \mathcal{A}_{\mathcal{R}} \in \mathcal{Q}_E(n_B, \mu) \left(\frac{k}{aH}\right)^{n_B-3} e^{-\mu N_t(n_B-6)}, \quad (5.37)$$

where

$$\begin{aligned} \mathcal{Q}_B(n_B, \mu) &= \frac{2^{3-n_B}}{\pi^3} \Gamma^2\left(\frac{6-n_B}{2}\right) |1+\mu|^{5-n_B}, \\ \mathcal{Q}_E(n_B, \mu) &= \frac{2^{5-n_B}}{\pi^3} \Gamma^2\left(\frac{8-n_B}{2}\right) |1+\mu|^{7-n_B}, \end{aligned} \quad (5.38)$$

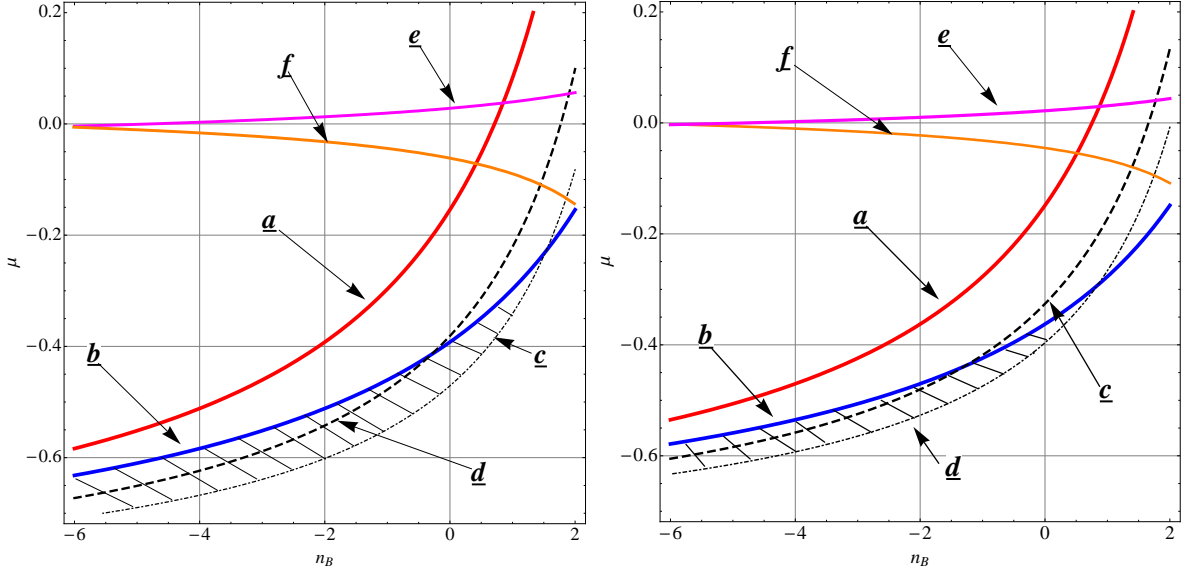


Figure 4: The exclusion plot in the case $\sigma < 0$. As in Figs. 2 the shaded area illustrates the allowed region in the parameter space where the magnetogenesis requirements are met and the back-reaction constraints satisfied.

The scale-invariant magnetic power spectrum occurs for $n_B = 1$:

$$\Omega_B(k, N_t, 1, \mu) = \frac{8\pi^2}{3} \mathcal{A}_R \epsilon \mathcal{Q}_B(1, \mu) e^{3\mu N_t}, \quad (5.39)$$

$$\Omega_E(k, N_t, 1, \mu) = \frac{8\pi^2}{3} \mathcal{A}_R \epsilon \mathcal{Q}_E(1, \mu) \left(\frac{k}{aH}\right)^{-2} e^{5\mu N_t}. \quad (5.40)$$

The scale-invariant electric power spectrum occurs for $n_B = 3$:

$$\Omega_B(k, N_t, 3, \mu) = \frac{8\pi^2}{3} \mathcal{A}_R \epsilon \mathcal{Q}_B(3, \mu) \left(\frac{k}{aH}\right)^2 e^{\mu N_t}, \quad (5.41)$$

$$\Omega_E(k, N_t, 3, \mu) = \frac{8\pi^2}{3} \mathcal{A}_R \epsilon \mathcal{Q}_E(3, \mu) e^{3\mu N_t}. \quad (5.42)$$

By looking at Eqs. (5.39)–(5.40) and (5.41)–(5.42) it can be argued that μ must be negative to have compatibility of the spectra with the critical density bound. This conclusion is corroborated by the exclusion plot in the (μ, n_B) plane which is illustrated in Fig. 4 where the shaded area represents the allowed region in the parameter space where the magnetogenesis requirements are met and the back-reaction constraints satisfied both at large and small scales. The various labels on the curves have the same meaning of the ones already discussed in connection with Fig. 2.

The results of Fig. 4 can be considered in conjunction with the ones of Fig. 1. If $\sigma < 0$ the relation of σ and n_B implies that the electric and magnetic susceptibilities are both decreasing provided the following pair of inequalities is satisfied:

$$n_B < \frac{8\mu + 7}{\mu + 1}, \quad n_B < \frac{6\mu + 7}{\mu + 1}, \quad (5.43)$$

where first inequality refers to χ_B while the second to χ_E . If $\mu < -1$ the first inequality is always verified since $n_B < 6$ and the asymptote of the first hyperbola is $n_B = 8$; the second inequality may or may not be verified. Therefore, for $\mu < -1$ and $n_B < 6$, χ_B is always decreasing while χ_E may either increase or decrease. If $\mu > -1$ we have somehow an opposite situation so that the second inequality of Eq. (5.43) is always verified while the first inequality may or may not be verified; furthermore, since $n_B = 6$ intersects the first hyperbola in $\mu = -1/2$ we must have $-1 < \mu < -1/2$. This means that χ_E is always decreasing while χ_B may or may not decrease.

We can therefore summarize by saying that in the shaded area of Fig. 4 it is possible to find viable models of magnetogenesis in two complementary cases, i.e. *either when the susceptibilities are both decreasing during the quasi-de Sitter stage or when one of the susceptibilities increases and the other decreases.*

5.7 Side remarks and specific cases

The borderline situations $\sigma = 0$ and $\sigma = 1$ must be separately discussed. If $\sigma = 0$ the power spectra of Eqs. (4.16) and (4.17) are, up to logarithmic corrections, $P_B \propto H^4 x^5 y^{2\mu}$ and $P_E \propto H^4 x^3$. If $\sigma = 1$ we have, by duality, $P_B(x, y, \mu, 1) = P_E(x, y, \mu, 0)$ and $P_E(x, y, \mu, 1) = P_B(x, y, \mu, 0)$. None of these two cases is particularly relevant from the phenomenological viewpoint.

In Fig. 2 the region of the parameter space where $\mu \rightarrow 0$ is allowed: whenever $\mu \rightarrow 0$ there is a region in the parameter space where the two susceptibilities coincide, the back-reaction constraints are avoided and the magnetogenesis constraints satisfied. This is consistent with earlier results (see, e.g. [12, 22]). The same exercise can be done in the case of Fig. 4 where the situation is different since the region of the parameter space with $\mu = 0$ is not included in the allowed region of the parameter space. This is a further evidence that the parameter space of the model is wider when the two susceptibilities do not coincide.

6 Concluding remarks

In this paper we investigated the possibility that the electric and the magnetic susceptibilities do not coincide during a phase of quasi-de Sitter expansion. Using a generalized duality symmetry it is possible to relate the electric and the magnetic power spectra of the quantum fluctuations. The parameter space of inflationary magnetogenesis is widened in comparison with the conventional situation where the susceptibilities are equal. The minimal magnetogenesis requirements are met in various regions of the parameter space where back-reaction effects are absent. The magnetic fields can be as large as $\mathcal{O}(0.01)$ nG for typical scales $\mathcal{O}(\text{Mpc})$. Both strongly coupled and weakly coupled initial conditions are possible but with different spectral features.

References

- [1] K. Enqvist, Int. J. Mod. Phys. D **07**, 331 (1998).
- [2] M. Giovannini, Int. J. Mod. Phys. D **13**, 391 (2004); Class. Quant. Grav. **23**, R1 (2006).
- [3] J. D. Barrow, R. Maartens and C. G. Tsagas, Phys. Rept. **449**, 131 (2007).
- [4] M. Giovannini, Phys. Rev. D **62**, 123505 (2000).
- [5] B. Ratra, Astrophys. J. Lett. **391**, L1 (1992).
- [6] M. Gasperini, M. Giovannini, and G. Veneziano, Phys. Rev. Lett. **75**, 3796 (1995);
M. Giovannini, Phys. Rev. D **56**, 3198 (1997).
- [7] M. Giovannini, Phys. Rev. D **64**, 061301 (2001).
- [8] K. Bamba and M. Sasaki, JCAP **02**, 030 (2007); K. Bamba JCAP **10**, 015 (2007).
- [9] M. Giovannini, Phys. Lett. B **659**, 661 (2008).
- [10] K. Bamba, Phys. Rev. D **75** 083516 (2007); J. Martin and J. 'i. Yokoyama, JCAP **0801**,
025 (2008); M. Giovannini, Lect. Notes Phys. **737**, 863 (2008); S. Kanno, J. Soda and
M. -a. Watanabe, JCAP **0912**, 009 (2009).
- [11] I. A. Brown, Astrophys. J. **733**, 83 (2011); N. Barnaby, R. Namba and M. Peloso, Phys.
Rev. D **85**, 123523 (2012); C. Bonvin, C. Caprini and R. Durrer, Phys. Rev. D **86**,
023519 (2012); T. Fujita and S. Mukohyama, JCAP **1210**, 034 (2012); T. Kahniashvili,
A. Brandenburg, L. Campanelli, B. Ratra and A. G. Tevzadze, Phys. Rev. D **86**, 103005
(2012).
- [12] M. Giovannini, Phys. Rev. D **85**, 101301 (2012); Phys. Rev. D **86**, 103009 (2012); Phys.
Rev. D **87**, 083004 (2013).
- [13] M. Giovannini, Class. Quantum Grav. **30**, 205017 (2013); Phys. Rev. D **87**, 083004
(2013).
- [14] A. R. Liddle, A. Mazumdar and F. E. Schunck, Phys. Rev. D **58**, 061301 (1998);
E. J. Copeland, A. Mazumdar and N. J. Nunes, Phys. Rev. D **60**, 083506 (1999);
A. A. Coley and R. J. van den Hoogen, Phys. Rev. D **62**, 023517 (2000).
- [15] G. Feinberg and J. Sucher, Phys. Rev. A **2**, 2395 (1970).
- [16] R. D. Peccei and H. R. Quinn, Phys. Rev. Lett. **38**, 1440 (1977); Phys. Rev. D **16**,
1791 (1977); J. Kim, Phys. Rep. **150**, 1 (1987); H.-Y. Cheng, *ibid.*, **158**, 1 (1988); G. G.
Raffelt, Phys. Rep. **198**, 1 (1990); Lect. Notes Phys. **741**, 51 (2008).

- [17] S. Carroll, G. Field and R. Jackiw, Phys. Rev. D **41**, 1231 (1990); W. D. Garretson, G. Field and S. Carroll, Phys. Rev. D **46**, 5346 (1992); G. Field and S. Carroll Phys.Rev.D **62**, 103008 (2000).
- [18] K. Bamba, Phys. Rev. D **74**, 123504 (2006); K. Bamba, C. Q. Geng and S. H. Ho, Phys. Lett. B **664**, 154 (2008).
- [19] L. Campanelli, Int. J. Mod. Phys. D **18**, 1395 (2009); L. Campanelli and M. Giannotti, Phys. Rev. D **72**, 123001 (2005); Phys. Rev. Lett. **96**, 161302 (2006).
- [20] M. Giovannini, Phys. Rev. D **61**, 063502 (2000); Phys. Rev. D **61**, 063004 (2000); “*Anomalous magnetohydroynamics*,” CERN-TH-PH/2013-152, arXiv:1307.2454 [hep-th].
- [21] S. Deser and C. Teitelboim, Phys. Rev. D **13**, 1592 (1976); S. Deser, J. Phys. A **15**, 1053 (1982).
- [22] M. Giovannini, JCAP **1004**, 003 (2010).
- [23] A. Lichnerowicz, *Magnetohydrodynamics: Waves and Shock Waves in Curved Space-time*, (Kluwer academic publisher, Dordrecht, 1994).
- [24] M. Giovannini, Class. Quant. Grav. **21**, 4209 (2004); last paper of Ref. [12]; R. J. Z. Ferreira, R. K. Jain and M. S. Sloth, arXiv:1305.7151 [astro-ph.CO].
- [25] S. Weinberg, *Cosmology* (Oxford University Press, Oxford 2008), p. 201.
- [26] M. Novello and S.E. Perez Bergliaffa, Phys. Rep. **463**, 127 (2008).
- [27] M. Abramowitz and I. A. Stegun, *Handbook of Mathematical Functions* (Dover, New York, 1972).
- [28] A. Erdelyi, W. Magnus, F. Obethtinger, and F. Tricomi, *Higher Transcendental Functions* (Mc Graw-Hill, New York, 1953).
- [29] G. Hinshaw, *et al.*, arXiv:1212.5226 [astro-ph.CO]; C. L. Bennett, *et al.*, arXiv:1212.5225 [astro-ph.CO].
- [30] C. L. Bennett *et al.*, Astrophys. J. Suppl. **192**, 17 (2011); N. Jarosik *et al.*, Astrophys. J. Suppl. **192**, 14 (2011); J. L. Weiland *et al.*, Astrophys. J. Suppl. **192**, 19 (2011); D. Larson *et al.*, Astrophys. J. Suppl. **192**, 16 (2011); B. Gold *et al.*, Astrophys. J. Suppl. **192**, 15 (2011); E. Komatsu *et al.*, Astrophys. J. Suppl. **192**, 18 (2011).
- [31] D. N. Spergel *et al.*, Astrophys. J. Suppl. **170**, 377 (2007); D. N. Spergel *et al.* Astrophys. J. Suppl. **148**, 175 (2003).

- [32] D. J. Eisenstein *et al.* [SDSS Collaboration], *Astrophys. J.* **633**, 560 (2005); W. J. Percival, *et al.* *Mon. Not. Roy. Astron. Soc.* **381**, 1053 (2007).
- [33] A. G. Riess *et al.* [Supernova Search Team Collaboration], *Astrophys. J.* **607**, 665 (2004); B. J. Barris *et al.*, *Astrophys. J.* **602**, 571 (2004); P. Astier *et al.* [The SNLS Collaboration], *Astron. Astrophys.* **447**, 31 (2006).
- [34] M. Hicken *et al.*, *Astrophys. J.* **700**, 1097 (2009); A. Conley *et al.*, *Astrophys. J. Suppl.* **192**, 1 (2011); M. Sullivan *et al.*, *Astrophys. J.* **737**, 102 (2011).
- [35] W. J. Percival *et al.* [SDSS Collaboration], *Mon. Not. Roy. Astron. Soc.* **401**, 2148 (2010).
- [36] J. Dunkley, R. Hlozek, J. Sievers, V. Acquaviva, P. A. R. Ade, P. Aguirre, M. Amiri and J. W. Appel *et al.*, *Astrophys. J.* **739**, 52 (2011).
- [37] R. Keisler, C. L. Reichardt, K. A. Aird, B. A. Benson, L. E. Bleem, J. E. Carlstrom, C. L. Chang and H. M. Cho *et al.*, *Astrophys. J.* **743**, 28 (2011).
- [38] J. Guy, M. Sullivan, A. Conley, N. Regnault, P. Astier, C. Balland, S. Basa and R. G. Carlberg *et al.* *Astron. Astrophys.* **523**, A7 (2010).
- [39] M. Giovannini, *Phys. Rev. D* **60**, 123511 (1999); A. R. Liddle and S. M. Leach, *Phys. Rev.* **D68**, 103503 (2003).
- [40] H. Heiselberg, *Phys. Rev. D* **49**, 4739 (1994); J. Ahonen and K. Enqvist, *Phys. Lett. B* **382**, 40 (1996); J. Ahonen, *Phys. Rev. D* **59**, 023004 (1999).